A New Family of Chelating Diphosphines with a Transition Metal Stereocenter in the Backbone: Novel Applications of "Chiral-at-Rhenium" Complexes in Rhodium-Catalyzed Enantioselective Alkene Hydrogenations

Klemenz Kromm,[a] Bill D. Zwick,[b] Oliver Meyer,[b] Frank Hampel,[a] and John A. Gladysz*[a]

Abstract: The title compounds are accessed by sequences starting with racemic and enantiomerically pure [(η^5-C_5H_5)Re(NO)(PPh_3)(CH_3)]. Reactions with chlorobenzene/HBF_4, PPh_2H, and *t*BuOK give the phosphido complex [(η^5-C_5H_5)Re(NO)(PPh_3)(PPh_2)] (**3**). Reactions with $Ph_3C^+BF_4^-$, PPh_2H, and *t*BuOK give the methylene homologue [(η^5-C_5H_5)Re(NO)(PPh_3)(CH_2PPh_2)] (**9**). Treatment of **3** or **9** with *n*BuLi or *t*BuLi and then PPh_2Cl gives the diphosphido systems [(η^5-$C_5H_4PPh_2$)Re(NO)(PPh_3)-((CH_2)$_n$$PPh_2$)] ($n = 0/1$, **5**/**11**). Reactions of **5** and **11** with [Rh(NBD)Cl]$_2$/$AgPF_6$ (NBD = norbornadiene) give the rhenium/rhodium chelate complexes [(η^5-C_5H_4-PPh_2)Re(NO)(PPh_3)((μ-CH_2)$_n$$PPh_2$)Rh-(NBD)]$^+$ PF_6^- ($n = 0/1$, **6**$^+$/**12**$^+$ PF_6^-; 30–32% overall from commercial $Re_2(CO)_{10}$). The crystal structures of **6**$^+$ PF_6^- and **12**$^+$ PF_6^- are compared to those of **3** and **9**, and other rhodium complexes of chelating bis(diphenylphosphines). The chiral pockets defined by the PPh_2 groups show unusual features. Four alkenes of the type (*Z*)-RCH=C(NHCOCH$_3$)CO$_2$R′ are treated with H_2 (1 atm) and (*R*)-**6**$^+$ PF_6^- or (*S*)-**12**$^+$ PF_6^- (0.5 mol%) in THF at room temperature. Protected amino acids are obtained in 70–98% yields and 93–82% *ee* [(*R*)-**6**$^+$ PF_6^-] or 72–60% *ee* [(*S*)-**12**$^+$ PF_6^-]. Pressure and temperature effects are defined, and turnover numbers of >1600 are realized.

Keywords: asymmetric hydrogenation · amino acids · catalyst · conformation analysis · heterobimetallic

Introduction

The design of new enantioselective catalysts is both an art and a science. For inspiration, chemists have considered virtually every type of chiral building block available in non-racemic form.[1, 2] For example, the use of metal catalysts featuring ferrocene-based chelating ligands with "planar chirality" has grown rapidly over the last decade.[3, 4] Many have proved spectacularly successful, and two representative ligand classes are illustrated in Scheme 1 (**A**, **A′**). This led us to speculate that chelating ligands that incorporate a chiral metal center—for example, a non-planar spectator moiety of general formula M(A)(B)(C)(D)—might also provide efficient and perhaps superior stereogenesis. We thought that the chelate backbone would be a particularly favorable position for such a group, as represented schematically by **B** in Scheme 1.

Such ligands can be viewed as relatives of classical chiral chelates such as DIOP and chiraphos,[5] with the carbon stereocenters replaced by a metal stereocenter. They offer a number of potential advantages. First, metal-based stereocenters constitute extremely flexible diversity elements. Second, steric properties can be fine-tuned in numerous ways. Third, electronic effects of metals are often transmitted over considerable distances,[6] and could be employed to either stabilize or (hemi)labilize a chelate. One concern might be whether metal-containing ligands will be as robust as carbon analogues. However, ferrocenes are sensitive towards electrophiles and oxidizing agents, but chelating ligands of the types **A**/**A′** yield metal catalysts that give very high turnover numbers and are applied in industrial processes.[3a,e]

The field of "chiral-at-metal" complexes has been pioneered by H. Brunner.[7] Several enantioselective catalysts bearing a M(A)(B)(C)(D) substructure or active site have been reported, but all examples to date contain additional carbon stereocenters.[2, 7, 8] We have conducted extensive studies of

[a] Prof. Dr. J. A. Gladysz, Dipl.-Chem. K. Kromm, Dr. F. Hampel
Institut für Organische Chemie
Universität Erlangen-Nürnberg
Henkestrasse 42, 91054 Erlangen (Germany)
E-mail: gladysz@organik.uni-erlangen.de

[b] Dr. B. D. Zwick, Dr. O. Meyer
Department of Chemistry, University of Utah
Salt Lake City, Utah 84112 (USA)

Supporting information for this article is available on the WWW under http://www.wiley-vch.de/home/chemistry/ or from the author.

  0947-6539/01/0709-2015 $ 17.50+.50/0

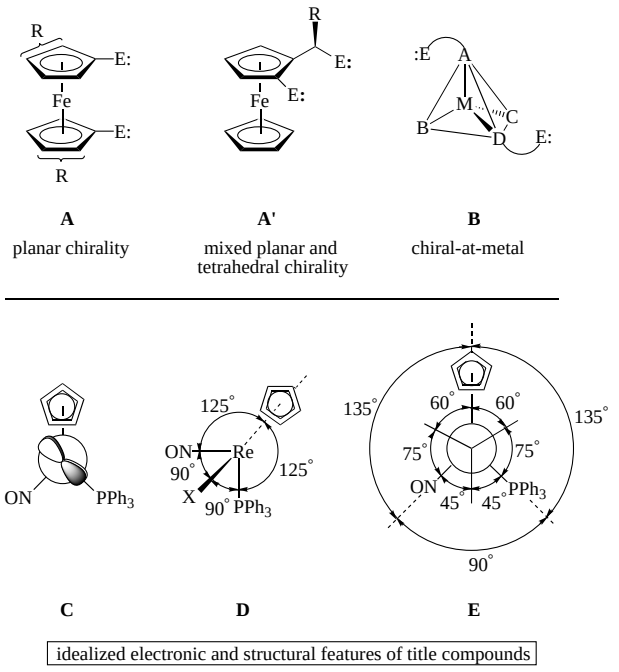

Scheme 1. Chiral organometallic scaffolds for chelating ligands.

chiral rhenium complexes of the formula $[(\eta^5\text{-}C_5H_5)Re(NO)(PPh_3)(X)]$ (see **C**–**E** in Scheme 1). These are easily obtained in enantiomerically pure form[9] and with only a few exceptions (X = OR, NR_2) are configurationally robust at ambient temperature.[10] However, most of the enantioselective organic transformations developed to date have been stoichiometric in rhenium.[11] In view of the flexibility with which this template can be elaborated—virtually any type of X group is possible, other phosphorus donor ligands can be employed, and substituted cyclopentadienyl ligands can be introduced—we set out to incorporate it into chelate ligands of the type **B** (Scheme 1).

Some key properties of these compounds deserve emphasis at the outset. First, the sixteen-valence-electron fragment $[(\eta^5\text{-}C_5H_5)Re(NO)(PPh_3)]^+$ is both a Lewis acid and a strong π base, with the d-orbital HOMO shown in **C**. This is a key determinant of conformation in adducts of unsaturated ligands (attractive interactions)[12] and saturated ligands with lone pairs on the ligating atom (repulsive interactions).[13] Second, such complexes are formally octahedral, with the cyclopentadienyl ligand occupying three coordination sites as shown in **D**. Thus, there are small but sometimes important differences in bond and torsion angle relationships as compared to carbon stereocenters, some of which are evident in **E**. Third, the basicity and nucleophilicity of any lone pair on the ligating atom X is enhanced relative to organic analogues.[13, 14] This has been most clearly documented with phosphido complexes $[(\eta^5\text{-}C_5H_5)Re(NO)(PPh_3)(PR_2)]$, which are alkylated by CH_2Cl_2 at room temperature,[13] and has its main origin in the rhenium/lone pair repulsive interactions noted above. Fourth, this effect persists with ligands of the type -CH_2X', as most clearly demonstrated for sulfur-containing species.[15]

There is an extensive literature of enantioselective catalysts bearing chelating diphosphine ligands.[1–5, 16] In view of the many benchmarks available, coupled with numerous unsolved problems relating to enantiomeric excesses, rates, and yields, we began our efforts in this area. In the narrative below, we describe new enantioselective alkene hydrogenation catalysts that provide a convincing proof-of-concept. Additional applications of our ligand systems will reported elsewhere.[17] A small portion of this work has been communicated.[18]

Results

Non-racemic five-membered chelates: The non-racemic methyl complex (S)-$[(\eta^5\text{-}C_5H_5)Re(NO)(PPh_3)(CH_3)]$, [(*S*)-**1**],[19, 20] was prepared from commercial $Re_2(CO)_{10}$ in a routine series of steps as previously described.[9] An enantiomeric purity of >99% *ee* was verified by HPLC.[21] As shown in Scheme 2, (*S*)-**1** and etheral HBF_4 were combined in chlorobenzene at −41 °C. This generates a substitution-labile,

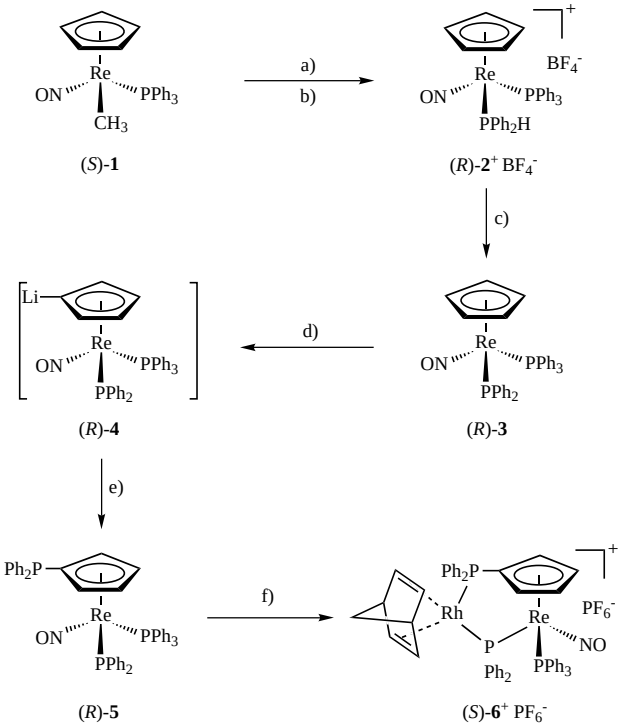

Scheme 2. Synthesis of the non-racemic five-membered chelating diphosphine.[19] a) Chlorobenzene, HBF_4, −41 °C; b) PPh_2H; c) *t*BuOK, THF, 25 °C; d) *n*BuLi, THF, −78 °C; e) PPh_2Cl, THF, −78 °C; f) $[Rh(NBD)Cl]_2$, $AgPF_6$, THF, 20 °C.

cationic chlorobenzene adduct that serves as a functional equivalent of the chiral Lewis acid $[(\eta^5\text{-}C_5H_5)Re(NO)(PPh_3)]^+$.[22] Addition of PPh_2H gave the diphenylphosphine complex (R)-$[(\eta^5\text{-}C_5H_5)Re(NO)(PPh_3)(PPh_2H)]^+$ BF_4^-, [(*R*)-**2**$^+$ BF_4^-], in 89% yield after workup. The racemic tosylate salt **2**$^+$ OTs^- has been prepared by a related route.[13a, 23] Reaction of (*R*)-**2**$^+$ BF_4^- and *t*BuOK as previously described for **2**$^+$ OTs^- gave the diphenylphosphido complex (R)-$[(\eta^5$-

0947-6539/01/0709-2016 $ 17.50+.50/0 *Chem. Eur. J.* **2001**, *7*, No. 9

C_5H_5)Re(NO)(PPh_3)(PPh_2)], [(*R*)-**3**], in 99% yield after workup.

Complexes (*R*)-**2**$^+$ BF_4^- and (*R*)-**3** exhibited good thermal stabilities. However, the latter was very air sensitive in solution and the solid state, analogous to the racemate, which gives a ReP(=O)Ph_2 species.[13a] The rhenium configurations, both corresponding to retention, were assigned by analogy to many closely related reactions.[10, 12, 22, 24] Standard methods for assaying enantiomeric purities were not successful. However, complete retention is normally observed. The hydrogenation enantioselectivities described below also require very high enantiomer ratios. The $^{31}P\{^1H\}$ NMR spectra of all new complexes are summarized in Table 1. The PPh_3 signals of

Table 1. Summary of $^{31}P\{^1H\}$ NMR data.[a]

Complex	$RePPh_3$	$Re(CH_2)_nPPh_2X$	$C_5H_4PPh_2X'$
2$^+$ BF_4^-[b,g]	13.3 (d)	−5.5 (d)	–
	^2J(P,P) = 13 Hz	^2J(P,P) = 13 Hz	
3[d,g]	19.5 (d)	−48.3 (d)	–
	^2J(P,P) = 15 Hz	^2J(P,P) = 15 Hz	
4[d,g,i]	21.6 (d)	−41.2 (d)	–
	^2J(P,P) = 16 Hz	^2J(P,P) = 16 Hz	
5[d,g]	20.2 (d)	−45.2 (d)	−16.2 (s)
	^2J(P,P) = 15 Hz	^2J(P,P) = 15 Hz	
6$^+$ PF_6^-[b,f,g]	9.8 (dd)	−49.2 (ddd)	50.4 (ddd)
	^2J(P,P) = 14 Hz,	^1J(P,Rh) = 127 Hz,	^1J(P,Rh) = 183 Hz,
	^3J(P,P) = 5 Hz	^2J(P,P) = 19 Hz,	^2J(P,P) = 19 Hz,
		^2J(P,P) = 14 Hz	^3J(P,P) = 5 Hz
14[b,g]	26.1 (s)	–	−14.9 (s)
8$^+$ BF_4^-[b,h]	21.7 (d)	30.2 (d)	–
	^3J(P,P) = 12 Hz	^3J(P,P) = 12 Hz	
9[e,h]	25.8 (d)	8.1 (d)	–
	^3J(P,P) = 8 Hz	^3J(P,P) = 8 Hz	
10[d,h,i]	28.3 (d)	10.0 (d)	–
	^2J(P,P) = 16 Hz	^2J(P,P) = 16 Hz	
11[c,h]	26.3 (d)	6.9 (dd)	−17.7 (d)
	^3J(P,P) = 8 Hz	^3J(P,P) = 3 Hz,	^3J(P,P) = 3 Hz
		^3J(P,P) = 8 Hz	
12$^+$ PF_6^-[e,f,h]	20.2 (dd)	50.5 (ddd)	23.9 (ddd)
	^3J(P,P) = 18 Hz,	^1J(P,Rh) = 148 Hz,	^1J(P,Rh) = 166 Hz,
	^3J(P,P) = 4 Hz	^2J(P,P) = 34 Hz,	^2J(P,P) = 34 Hz,
		^3J(P,P) = 18 Hz	^3J(P,P) = 4 Hz

[a] At room temperature unless noted. [b] In CD_2Cl_2. [c] In C_6D_6. [d] In THF. [e] In $CDCl_3$. [f] PF_6^- −144.0 (sep, ^1J(P,F) = 708 Hz). [g] 121 MHz. [h] 162 MHz. [i] At −80 °C.

(*R*)-**2**$^+$ BF_4^- and (*R*)-**3** were in normal ranges for this series of compounds, and coupled to the other ligating phosphorus with ^2J(P,P) values of 13–15 Hz. Other NMR (^1H, ^{13}C), as well as IR, microanalytical, and polarimetric data are given in the Experimental Section.

The cyclopentadienyl ligand of methyl complex **1** can be lithiated and then alkylated.[25] As shown in Scheme 2, a similar sequence was investigated for elaborating (*R*)-**3** to a chelating diphosphine. Reaction with *n*BuLi (1.1 equiv, −78 °C) in THF gave a deep red solution, and a $^{31}P\{^1H\}$ NMR spectrum of an aliquot (Table 1) showed the clean formation of a species that was assigned as the lithiocyclopentadienyl complex (*R*)-[(η^5-C_5H_4Li)Re(NO)(PPh_3)(PPh_2)], (*R*)-**4**. It persisted, in separate experiments, for several days in solution at room temperature. Addition of PPh_2Cl (1.0 equiv) and workup gave the target diphenylphosphidocyclopentadienyl complex (*R*)-[(η^5-$C_5H_4PPh_2$)Re(NO)(PPh_3)(PPh_2)], [(*R*)-**5**], in 89% yield as a spectroscopically pure red foam.

Crystallization of (*R*)-**5** from benzene/hexane gave red prisms of a benzene hemisolvate. Racemic **5** was prepared by a separate route described below. The ^1H and $^{13}C\{^1H\}$ NMR spectra showed patterns characteristic of η^5-C_5H_4X ligands.[26] The $^{31}P\{^1H\}$ spectrum showed three signals (Table 1), with the $C_5H_4PPh_2$ resonance not detectably coupled to the rhenium-bound phosphorus atoms. When this synthesis was conducted with an excess of PPh_2Cl, a by-product formed. The $^{31}P\{^1H\}$ NMR data suggested a species with a $RePPh_2PPh_2$ linkage.

In a standard protocol for the synthesis of rhodium complexes of chelating diphosphines,[27] (*R*)-**5**, the rhodium norbornadiene complex $[Rh(NBD)Cl]_2$,[23b] and $AgPF_6$ were combined in THF at room temperature. As shown in Scheme 2, workup gave the heterobimetallic rhenium/rhodium complex (*S*)-[(η^5-$C_5H_4PPh_2$)Re(NO)(PPh_3)(μ-PPh_2)Rh(NBD)]$^+$ PF_6^-, [(*S*)-**6**$^+$ PF_6^-], as a dark orange powder and THF hemisolvate in 92% yield. The structure followed readily from the spectroscopic properties. Most diagnostic was the richly featured $^{31}P\{^1H\}$ NMR spectrum summarized in Table 1 (and illustrated elsewhere).[18b] Both diphenylphosphido signals exhibited large ^1J(P,Rh) values (127, 183 Hz). The $C_5H_4PPh_2$ signal shifted downfield from that of precursor (*R*)-**5** (δ = 50.4 vs −16.2), and was coupled to both rhenium-bound phosphorus atoms. All crystallization attempts gave oils, but the crystal structure of the racemate is described below.

Six-membered chelates: We sought to compare a family of catalysts. Hence, a second, homologous, series of complexes was desired. One possibility was to retain the methyl carbon that was removed by protonation in the first step of Scheme 2. As shown in Scheme 3, either racemic or (*S*)-**1** and $Ph_3C^+BF_4^-$ were reacted in CH_2Cl_2 at −60 °C to generate the electrophilic methylidene complexes, racemic or (*S*)-[(η^5-C_5H_5)Re(NO)(PPh_3)(=CH_2)]$^+$ BF_4^-, (**7**$^+$ BF_4^-).[28] Then PPh_2H was added. Workups gave the new phosphonium salts, racemic or (*S*)-[(η^5-C_5H_5)Re(NO)(PPh_3)(CH_2PPh_2H)]$^+$ BF_4^-, (**8**$^+$ BF_4^-), as orange to red prisms in 95–98% yields. Similar syntheses of related cationic species with $ReCH_2PX_3$ linkages have been described.[29] Deprotonations with *t*BuOK gave the trivalent phosphines, racemic or (*S*)-[(η^5-C_5H_5)Re(NO)(PPh_3)(CH_2PPh_2)], (**9**), as orange to red needles in 91–89% yields.

Racemic or (*S*)-**8**$^+$ BF_4^- could be stored as solids in air for extended periods. Racemic or (*S*)-**9** were much less air sensitive than racemic or (*R*)-**3**, and solutions survived exposures of several hours. Thus, the additional methylene group attenuates the phosphorus lone pair reactivity. The $^{31}P\{^1H\}$ NMR spectra of **8**$^+$ BF_4^- and **9** showed ^3J(P,P) values that were 90–60% of the ^2J(P,P) values of **2**$^+$ BF_4^- and **3** (Table 1). The structures and configurations in Scheme 3 correspond to retention at rhenium. The addition of a carbon nucleophile to **7**$^+$ BF_4^- has been shown to proceed with retention.[29b] The absolute configuration of (*S*)-**9** is verified by a crystal structure below.

The conversion of racemic and (*S*)-**9** to diphenylphosphidocyclopentadienyl complexes was attempted next. Reactions

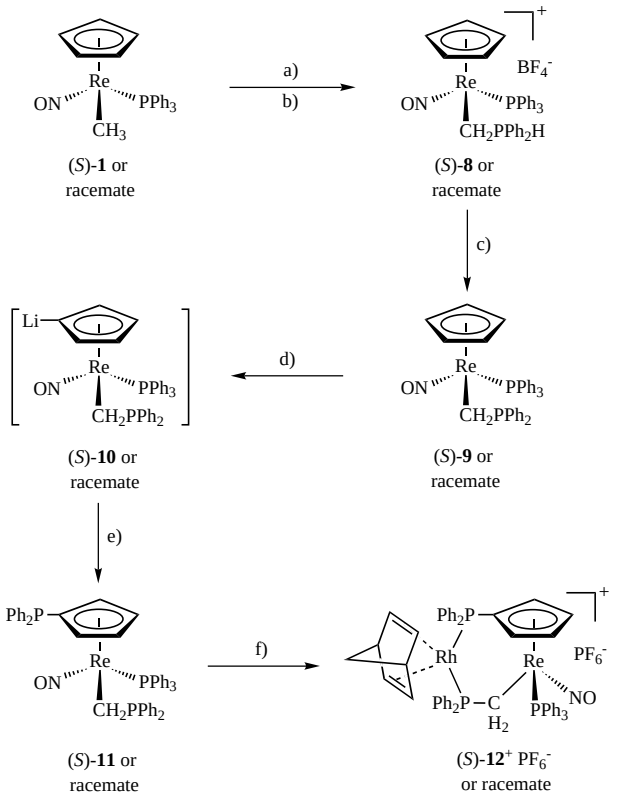

Scheme 3. Syntheses of the racemic and non-racemic six-membered chelating diphosphines. a) $Ph_3C^+BF_4^-$, CH_2Cl_2, $-60\,^\circ C$; b) PPh_2H, -60 to $25\,^\circ C$; c) *t*BuOK, THF, $25\,^\circ C$; d) *t*BuLi, THF, -60 to $-10\,^\circ C$; e) PPh_2Cl, THF, -78 to $25\,^\circ C$; f) $[Rh(NBD)Cl]_2$, $AgPF_6$, THF, $20\,^\circ C$.

with *t*BuLi (1.2 equiv, $\leq -30\,^\circ C$, then warming) in THF gave deep red solutions. The $^{31}P\{^1H\}$ NMR spectra of aliquots showed the clean formation of new signals (Table 1) that were attributed to the lithiocyclopentadienyl complexes, racemic and (*R*)-[(η^5-C_5H_4Li)Re(NO)(PPh_3)(CH_2PPh_2)] (**10**, Scheme 3). Additions of PPh_2Cl (1.0 equiv) and workups gave the target complexes, racemic and (*S*)-[(η^5-$C_5H_4PPh_2$)Re(NO)(PPh_3)(CH_2PPh_2)], (**11**), as orange-red solids in 70–68% yields. These could be exposed to air for brief periods, but were much more sensitive than the precursors, racemic and (*S*)-**9**. The $^{31}P\{^1H\}$ NMR spectrum of **11** (Table 1) was better resolved than that of lower homologue **5**, and only the $RePPh_3$ and $C_5H_4PPh_2$ signals were not detectably coupled.

Syntheses of rhodium chelate complexes were investigated. As shown in Scheme 3, racemic and (*S*)-**11** were treated with $[Rh(NBD)Cl]_2$ and $AgPF_6$. Workups gave the heterobimetallic rhenium/rhodium complexes, racemic and (*S*)-[(η^5-$C_5H_4PPh_2$)Re(NO)(PPh_3)(μ-CH_2PPh_2)Rh(NBD)]$^+$ PF_6^-, (**12**$^+$ PF_6^-), as brown or brownish red solids in 95–82% yields. These showed good air and thermal stabilities. The structures followed readily from the spectroscopic properties, the most diagnostic of which were the $^{31}P\{^1H\}$ NMR data (Table 1). Figure 1 compares the highly informative coupling patterns with those of precursor **11**. Both PPh_2Rh signals exhibit large ^1J(P,Rh) values, and are markedly downfield from their counterparts in **11**. Deep red prisms of a CH_2Cl_2 monosolvate of the racemate were obtained, and the crystal structure is described below.

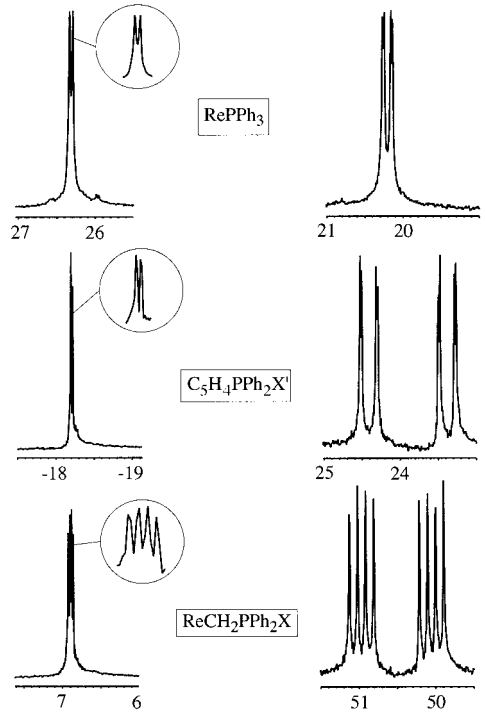

Figure 1. $^{31}P\{^1H\}$ NMR spectra of **11** (left) and **12**$^+$ PF_6^- (right).

Racemic five-membered chelates: The synthesis of (*S*)-**6**$^+$ PF_6^- in Scheme 2 represents a second-generation approach. The first generation approach, shown in Scheme 4, was initiated at a time when syntheses of adducts of [(η^5-C_5H_5)Re(NO)(PPh_3)]$^{n+}$ and phosphorus-donor ligands were still being optimized.[18b] It is described here because of certain

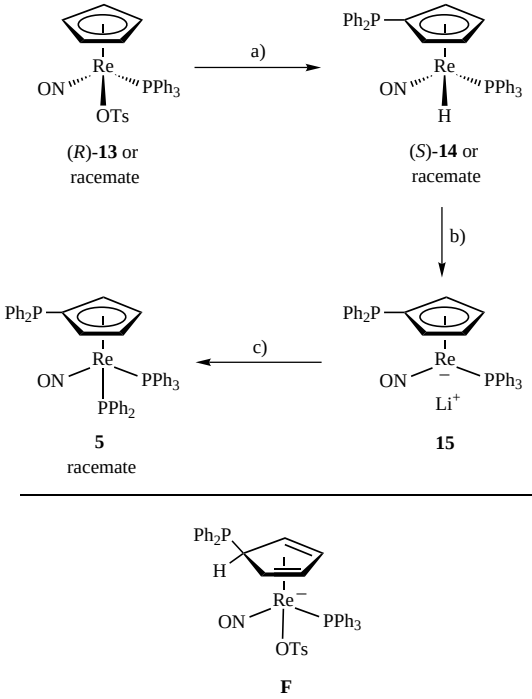

Scheme 4. Synthesis of the racemic five-membered chelating diphosphine **5**.[19] a) $LiPPh_2$, THF, $20\,^\circ C$, partial retention; b) *n*BuLi, THF, $-15\,^\circ C$; c) PPh_2Cl, THF, $-78\,^\circ C$.

0947-6539/01/0709-2018 $ 17.50+.50/0 *Chem. Eur. J.* **2001**, *7*, No. 9

novel features, and to accurately represent how some key data were obtained.

The tosylate complexes, racemic and (*R*)-[(η^5-C_5H_5)Re(NO)(PPh_3)(OTs)], (**13**),[19,30] were treated with $LiPPh_2$ in THF. The formation of diphenylphosphido complexes, racemic and (*R*)-**3**, was anticipated. Workups gave homogeneous products in high yields. However, the ^1H and ^{13}C NMR spectra showed patterns characteristic of η^5-C_5H_4X ligands.[25,26] The $^{31}P\{^1H\}$ NMR spectra (Table 1) exhibited two uncoupled signals, with chemical shifts close to those of the PPh_3 and $C_5H_4PPh_2$ ligands in **5** and **11**. The IR and ^1H NMR spectra showed plausible signals for hydride ligands ($\tilde{\nu}_{ReH} = 1950\,cm^{-1}$; $\delta = -9.56$) that closely matched those of the parent complex [(η^5-C_5H_5)Re(NO)(PPh_3)(H)].[31] Accordingly, the products were assigned to the structure [(η^5-$C_5H_4PPh_2$)Re(NO)(PPh_3)(H)] (**14**; 85–79%). The triflate complex [(η^5-C_5H_5)Re(NO)(PPh_3)(OTf)][23c,30] reacted under similar conditions to give a mixture of **3** and **14**.

Thus, the first step of Scheme 4 unexpectedly gave a diphenylphosphidocyclopentadienyl ligand that was, however, ultimately *desired*. Similar nucleophile-initiated sequences that lead to substituted cyclopentadienyl ligands and displacement of coordinated ligands by cyclopentadienyl-derived hydride have been reported.[32,33] From the limited data available, we presume that addition to the cyclopentadienyl ligand precedes hydride migration, as shown in structure **F** in Scheme 4. However, there is no precedent for the stereochemistry at the metal. The sample derived from (*R*)-**13** kept some optical activity ($[\alpha]_{589}^{22} = 89°$). The ORD spectrum was positive at 650–375 nm and negative at 375–250 nm, and the CD spectrum was positive at 650–450 nm and 425–275 nm and negative at 450–425 nm.[18b,19] This suggested dominant retention of configuration [(*S*)-**14**].[29b,30] However, the magnitude of the rotation is low for chiral rhenium compounds, and the enantiomeric purity could not be assayed.

The elaboration of the hydride ligand in **14** was attempted. The addition of *n*BuLi to the parent complex [(η^5-C_5H_5)Re(NO)(PPh_3)(H)] (THF, −15 °C) generates the red, rhenium-centered anion [(η^5-C_5H_5)Re(NO)(PPh_3)]$^-$ Li^+.[31] This in turn reacts with a variety of electrophiles to give new σ complexes. An analogous reaction of racemic **14** and *n*BuLi (Scheme 4) gave a deep red solution that was believed to contain [(η^5-$C_5H_4PPh_2$)Re(NO)(PPh_3)]$^-$ Li^+ (**15**). Addition of PPh_2Cl gave the diphenylphosphido complex **5** in 68% yield after workup. A sequence starting with the (*R*)-**14** of unknown enantiomeric purity also gave racemic **5**. This is in accord with earlier precedent,[31] and shows that the diphenylphosphido moiety does not impart any special configurational stability to **15**. Racemic **5** was converted to racemic **6**$^+$ PF_6^- as described for the non-racemic analogues in Scheme 2. Workup gave a THF monosolvate in 83% yield. Dark red prisms of a $CHCl_3$ disolvate were also obtained.

Catalyst structure: The crystal structures of (*S*)-**9**·C_6H_6 and the racemic rhenium-rhodium chelates **6**$^+$ PF_6^-·$(CHCl_3)_2$ and **12**$^+$ PF_6^-·CH_2Cl_2 were determined as outlined in Table 2 and the Experimental Section. The first is shown in Figure 2 (bottom), together with that previously found for the diphenylphosphido complex **3** (top).[13a] The structure confirms the absolute configuration, and the overall stereochemistry (retention) for the first two steps in Scheme 3. It also exhibits a LRe−CH_2X conformation similar to those of several related complexes.[15,29b,34] As illustrated by Newman-type projection **H** in Figure 3 (and quantified by the P1/N1-Re-C1-P2 torsion

Table 2. Crystallographic data.

	(*S*)-**9**·C_6H_6	**6**$^+$ PF_6^-·$(CHCl_3)_2$	**12**$^+$ PF_6^-·CH_2Cl_2
molecular formula	$C_{42}H_{38}NOP_2Re$	$C_{56}H_{49}Cl_6F_6NOP_4ReRh$	$C_{56}H_{51}Cl_2F_6NOP_4ReRh$
molecular weight	820.87	1461.65	1387.32
T[°C]	−100(2)	15	−100(2)
diffractometer	Nonius MACH3	Syntex P1-bar	Nonius MACH3
radiation [Å]	$Mo_{K\alpha}$	$Mo_{K\alpha}$	$Mo_{K\alpha}$
crystal system	monoclinic	monoclinic	monoclinic
space group	$P2_1$	$P2_1/c$	$P2_1/c$
unit cell dimensions:			
a [Å]	12.086(2)	12.980(4)	13.392(3)
b [Å]	8.559(2)	15.832(4)	11.155(2)
c [Å]	17.785(4)	29.117(7)	34.445(7)
β [°]	105.87(3)	91.70(3)	98.46(3)
V [Å^3]	1769.6(6)	5980.9(2)	5089.7(18)
Z	2	4	4
ρ_c [g cm^{-3}]	1.54	1.66	1.81
μ [mm^{-1}]	3.56	4.40	3.05
data collection method	Θ scans	Θ scans	Θ scans
crystal dimensions [mm]	0.2 × 0.2 × 0.2	0.3 × 0.3 × 0.3	0.4 × 0.4 × 0.3
Θ range [°]	≤25	≤25	≤25
range/indices (h,k,l)	−14,14;	0,15;	−15,15;
	−10,10;	0,16;	−13,13;
	−21,21	0,27	−40,40
reflections measured	5988	10957	18892
unique reflections	5290	10957	8951
reflections observed	4715 [$I > 2\sigma(I)$]	7201 [$I > 3\sigma(I)$]	6405 [$I > 2\sigma(I)$]
refined parameters	424	1269	649
refinement	least-squares on F^2	least-squares on F	least-squares on F^2
R_{int}	0.0392	–	0.0840
R indices	$R_1 = 0.0355$	$R = 0.0740$	$R_1 = 0.0404$
[$I > 2\sigma(I)$]	$wR_2 = 0.0842$	[R_w] = 0.0830	$wR_2 = 0.0807$
R indices (all data)	$R_1 = 0.0448$	–	$R_1 = 0.0801$
	$wR_2 = 0.0934$		$wR_2 = 0.1036$
goodness of fit	1.003	–	1.041
largest diff. peak, hole [e Å^{-3}]	2.184/−1.653	5.38[a]/–	1.838/−1.632

[a] 1.03 Å from Re.

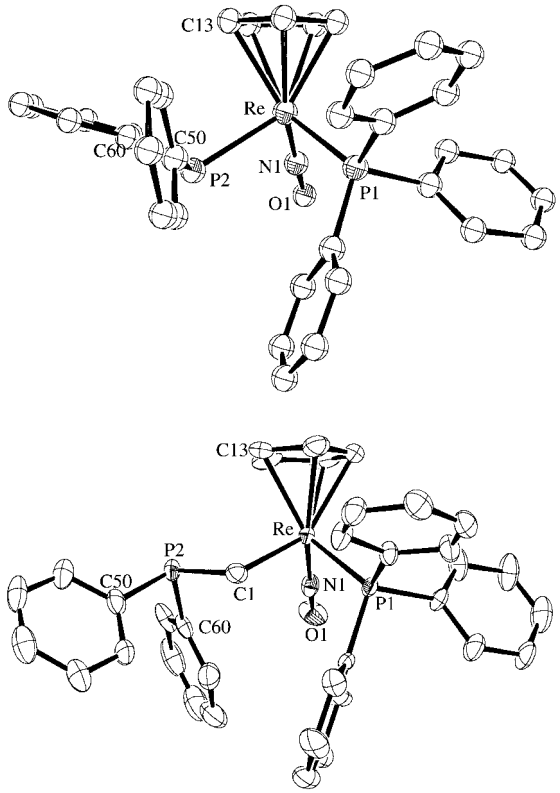

Figure 2. Molecular structure of **3** (top) and (*S*)-**9** C_6H_6 (bottom).

Table 3. Key distances [Å] and angles [°] in **3** and (*S*)-**9**·C_6H_6.

	3	(*S*)-**9**·C_6H_6
Re–N1	1.738(10)	1.773(7)
Re–P1	2.358(3)	2.352(2)
Re–P2	2.461(3)	–
Re–C1	–	2.170(8)
C1–P2	–	1.845(8)
Re–Cp(centroid)	1.944	1.949
Re–C13	2.287(16)	2.324(8)
N1-Re-P1	91.5(4)	92.5(2)
Re-N1-O1	177.9(10)	174.5(6)
C1-Re-C13	–	84.0(4)
P2-Re-C13	91.4(8)	–
N1-Re-C1	–	97.2(3)
N1-Re-P2	92.5(4)	–
P1-Re-C1	–	87.6(2)
P2-Re-P1	92.5(1)	–
Re-C1-P2	-	112.1(4)
P1-Re-C1-P2	–	– 159.9
N1-Re-C1-P2	–	– 67.6
Re-C1-P2-LP	–	– 49.1
Re-C1-P2-C50	–	– 176.9
Re-C1-P2-C60	–	78.8
P1-Re-P2-LP	60.7	–
N1-Re-P2-LP	30.9	–
P1-Re-P2-C50	62.6	–
P1-Re-P2-C60	175.9	–
N1-Re-P2-C50	154.3	–
N1-Re-P2-C60	– 92.5	–

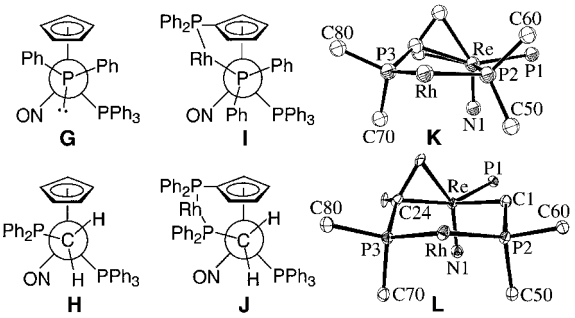

Figure 3. Selected conformational features in crystal structures.

angles in Table 3), the larger X group occupies the interstice between the cyclopentadienyl and nitrosyl ligands. Numerous NMR and computational data have shown this region to be the least congested.[35, 36]

In the crystal structure of **3** (Figure 2, top), the smallest group on the diphenylphosphido ligand, the lone pair, is directed into the interstice between the nitrosyl and triphenylphosphine ligands (see **G**, Figure 3). This is known to be the most congested region.[35] However, there is an additional electronic driving force. In this conformation, the torsion angle between the lone pair and rhenium fragment HOMO shown in **C** (Scheme 1) is about 60°. The high degree of orthogonality lessens repulsive interactions.[13a] Key metrical parameters of **3** and (*S*)-**9** are compared in Table 3. The effect of rhodium chelate formation upon these core structures is of obvious interest.

The structures of the cations of chelates **6**$^+$ PF_6^- and **12**$^+$ PF_6^- are shown in Figure 4. Selected distances and angles are compared in Table 4. With one exception (below), the bond lengths or angles common to both chelate rings are similar. For example, both PRhP angles are close to that expected for an idealized square planar rhodium geometry (91.35(12), 95.41(7) Å). However, the rhodium–rhenium distance is 10% greater in the larger six-membered ring (4.505 vs 4.068 Å). Protonation or alkylation of the phosphorus lone pair in **3** would relieve repulsive interactions and give a much shorter rhenium–phosphorus bond.[13b] However, the introduction of rhodium in **6**$^+$ PF_6^- leads to a slightly longer rhenium–phosphorus bond (2.487(3) vs 2.461(3) Å).

Newman-type projections of **6**$^+$ PF_6^- and **12**$^+$ PF_6^- are illustrated in Figure 3 (**I**, **J**). Due to the geometrical constraint of the chelate, the $LRePPh_2$ conformations of **3** and **6**$^+$ PF_6^- (**G**, **I**) differ significantly. However, since rhodium is now the largest group on phosphorus, that in **I** would be favored even in the absence of a chelate. In contrast, the $LReCH_2P$ conformations in (*S*)-**9** and **12**$^+$ PF_6^- (**H**, **J**) must change only slightly, as reflected by the torsion angles (L = Ph_3P/ON: – 159.9°/ – 67.6° vs – 157.3°/ – 68.3°). The situation with the adjacent $ReCH_2$–PPh_2 linkage is similar. Geometrical constraints require the rhodium in **J** to assume the phosphorus lone pair position in **H** (see also Figure 2, bottom).[36] Accordingly, the ReC–PPh torsion angles in (*S*)-**9** and **12**$^+$ PF_6^- are very close (78.8°/ – 176.9° vs 73.1°/179.4° or – 180.6°). However, the $ReCH_2$–PRh conformation is opposite to what would be expected in the absence of a chelate.[36b]

0947-6539/01/0709-2020 $ 17.50+.50/0 *Chem. Eur. J.* **2001**, *7*, No. 9

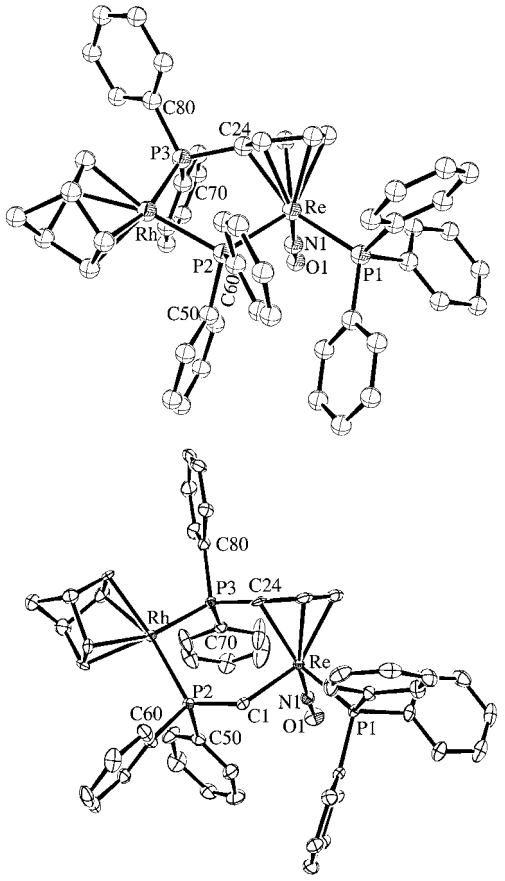

Figure 4. Structures of the cations of $\mathbf{6}^+\,PF_6^-\cdot(CHCl_3)_2$ (top) and $\mathbf{12}^+\,PF_6^-\cdot CH_2Cl_2$ (bottom).

Table 4. Key distances [Å] and angles [°] in $\mathbf{6}^+\,PF_6^-\cdot(CHCl_3)_2$ and $\mathbf{12}^+\,PF_6^-\cdot CH_2Cl_2$.

	$\mathbf{6}^+\,PF_6^-\cdot(CHCl_3)_2$	$\mathbf{12}^+\,PF_6^-\cdot CH_2Cl_2$
Re–N1	1.731(13)	1.760(7)
Re–P1	2.392(3)	2.365(2)
Re–P2	2.487(3)	–
Re–C1	–	2.183(7)
C1–P2	–	1.825(7)
Re–Cp(centroid)	1.925	1.939
Re–C24	2.217(12)	2.253(7)
P3–C24	1.805(12)	1.798(7)
Rh–P3	2.276(4)	2.295(2)
Rh–P2	2.380(3)	2.360(2)
Re–Rh	4.068	4.505
N1-Re-P1	90.8(3)	89.1(2)
N1-Re-C1	–	100.5(3)
N1-Re-P2	99.8(4)	–
C1-Re-P1	–	89.8(2)
P2-Re-P1	99.55(12)	–
Re-C1-P2	–	117.4(3)
Re-P2-Rh	113.4(3)	–
C24-Re-C1	–	99.4(3)
C24-Re-P2	87.4(3)	–
Rh-P2-C1	121.9(4)	–
Re-C24-P3	117.1(4)	123.3(3)
Rh-P3-C24	110.6(4)	113.9(3)
P2-Rh-P3	91.35(12)	95.41(7)
Rh-P2-C50	102.4(4)	113.3(2)
Rh-P2-C60	108.7(4)	108.5(2)
Rh-P3-C70	113.3(5)	111.0(2)
Rh-P3-C80	114.8(4)	115.1(2)
Re-C24-P3-C70	– 69.4	– 61.8
Re-C24-P3-C80	179.5	– 170.9
P1-Re-C1-P2	–	– 157.3
N1-Re-C1-P2	–	– 68.3
N1-Re-P2-C50	17.6	–
N1-Re-P2-C60	136.7	–
P1-Re-P2-C50	– 74.9	–
P1-Re-P2-C60	44.2	–
P1-Re-P2-Rh	167.2	–
Re-C1-P2-Rh	–	58.1
Re-C1-P2-C50	–	73.1
Re-C1-P2-C60	–	179.4

Figure 4 illustrates the overall conformation of the chelate rings in $\mathbf{6}^+\,PF_6^-$ and $\mathbf{12}^+\,PF_6^-$. A close inspection reveals an uncanny resemblance to the classical envelope and chair conformations of cyclopentane and cyclohexane, respectively. The similarities are highlighted in **K** and **L** in Figure 3. The latter features a striking array of three *syn*-axial phenyl and nitrosyl groups. We speculate that the essentially unrestricted rotation about the rhenium–cyclopentadienyl axis allows the $Re(CH_2)_nPRhP$ linkage to attain conformational energy minima similar to those of the corresponding carbocycles. Accordingly, the C24-Re-P2 and C24-Re-C1 angles, which reflect this degree of freedom, are quite different in the two chelates (87.4(3)° vs 99.4(3)°).

Views of $\mathbf{6}^+\,PF_6^-$ and $\mathbf{12}^+\,PF_6^-$ without the norbornadiene ligand are collected in Figure 5. An overlay (top) in which the chiral rhenium moieties are superimposed as closely as possible highlights the different chiral environments at rhodium. The chiral environments are then shown from the perspective of the ligands on rhodium (middle and bottom structures). Brunner has carefully analyzed such chiral pockets in complexes of chiral chelating bis(diphenylphosphines).[5a] He has classified the phenyl ring orientations into four types based upon torsion angle relationships: face–P, edge–P, edge–M, and face–M, where P and M are helical chirality descriptors.

Complexes $\mathbf{6}^+\,PF_6^-$ and $\mathbf{12}^+\,PF_6^-$ both feature two phenyl rings with face-orientations with respect to rhodium (upper quadrants in Figure 4). The phenyl rings in $\mathbf{6}^+\,PF_6^-$ define a P^3M pattern, which is found in only 10% of the five membered-chelates with envelope conformations of the same configuration (most are M^4 or M^3P).[5a] Furthermore, the phenyl ring containing C50 adopts a normally forbidden orientation, apparently to minimize interactions with the pseudoaxial nitrosyl group. In contrast, the phenyl rings in $\mathbf{12}^+\,PF_6^-$ adopt a P^2M^2 configuration. Derivations of these relationships are given as Supporting Information (Table 1-S). The most important point is that they validate our hypothesis that chelates of the type **B** (Scheme 1) should provide unique and heretofore inaccessible types of steric environments for enantioselective catalysts.

Catalytic enantioselective hydrogenations: Many chiral cationic rhodium diphosphine complexes have been evaluated as catalyst precursors for enantioselective hydrogenations of alkenes.[1, 4a,c–e, 16, 27a] Some are very effective with α,β-unsaturated carboxylic acids and esters that bear α-acetamido substituents. These afford products of obvious interest,

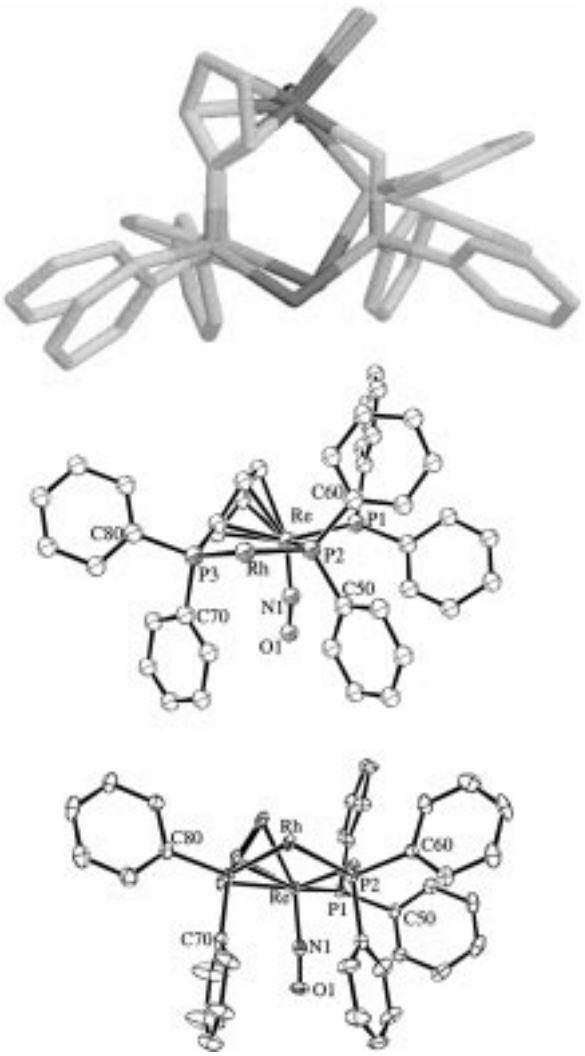

Figure 5. Top: Superposition of the cations of $\mathbf{6}^+\,PF_6^-\cdot(CHCl_3)_2$ and $\mathbf{12}^+\,PF_6^-\cdot CH_2Cl_2$, omitting the norbornadiene and PPh_3 phenyl rings. Middle and bottom: View of the chiral pockets of $\mathbf{6}^+$ and $\mathbf{12}^+$ from the perspective of ligands on rhodium, omitting the norbornadiene and one PPh_3 phenyl ring.

protected α-amino acids. As summarized in entries 1–8 of Table 5, four such substrates (**16a–d**) were treated with 1 atm of hydrogen in the presence of 0.5 mol% of the rhenium–rhodium chelates (*S*)-$\mathbf{6}^+\,PF_6^-$[19] and (*S*)-$\mathbf{12}^+\,PF_6^-$ in THF at ambient temperature. Workups gave the amino acid derivatives **17a–d** in 70–98% yields. All spectroscopic and chromatographic probes indicated quantitative reactions.

The absolute configurations of **17a–d** were assigned polarimetrically. The enantiomeric purities were determined by chiral chromatographic methods as described in the Experimental Section. The samples derived from (*S*)-$\mathbf{6}^+\,PF_6^-$ (entries 1–4) were first analyzed by GLC, and then stored for fourteen years and analyzed by GLC or HPLC. Compound **17a** in entry 1, originally reported as 98% *ee* from a non-baseline enantiomer separation,[18] was found to be 92% *ee*. The other values were in agreement. In all cases, the five-membered chelate, (*S*)-$\mathbf{6}^+\,PF_6^-$, gave higher *ee* values than the six-membered chelate, (*S*)-$\mathbf{12}^+\,PF_6^-$ (entries 1–4 vs 5–8).

Table 5. Catalytic enantioselective hydrogenation of dehydroamino acids.[a]

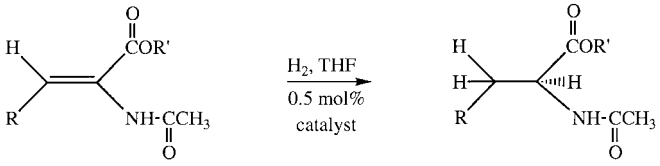

16 a-d a: R = H, R' = H; b: R = Ph, R' = H; c: R = Ph, R' = CH_3; d: R = Ph, R' = CH_2CH_3 (*S*)-**17 a-d**

Entry	Educt	Catalyst	*T* [°C]	Pressure [bar]	Yield [%]	*ee* [%]
1	**16a**	(*S*)-$\mathbf{6}^+\,PF_6^-$	20–23	1	82	92
2	**16b**	(*S*)-$\mathbf{6}^+\,PF_6^-$	20–23	1	70	93
3	**16c**	(*S*)-$\mathbf{6}^+\,PF_6^-$	20–23	1	94	88
4	**16d**	(*S*)-$\mathbf{6}^+\,PF_6^-$	20–23	1	86	82
5	**16a**	(*S*)-$\mathbf{12}^+\,PF_6^-$	20–23	1	93	62
6	**16b**	(*S*)-$\mathbf{12}^+\,PF_6^-$	20–23	1	86	72
7	**16c**	(*S*)-$\mathbf{12}^+\,PF_6^-$	20–23	1	98	65
8	**16d**	(*S*)-$\mathbf{12}^+\,PF_6^-$	20–23	1	96	60
9	**16b**	(*S*)-$\mathbf{12}^+\,PF_6^-$	20–23	0.3	–	76
10	**16b**	(*S*)-$\mathbf{12}^+\,PF_6^-$	20–23	10	–	60
11	**16b**	(*S*)-$\mathbf{12}^+\,PF_6^-$	20–23	30	–	46
12	**16b**	(*S*)-$\mathbf{12}^+\,PF_6^-$	20–23	90	–	40
14	**16b**	(*S*)-$\mathbf{12}^+\,PF_6^-$	–5	1	75	40
15	**16b**	(*S*)-$\mathbf{12}^+\,PF_6^-$	45	1	82	72

[a] Conditions and analytical methods are detailed in the Experimental Section.

This follows intuitively from the closer proximity of the chiral rhenium to one diphenylphosphido group and in turn the rhodium.

The effect of hydrogen pressure upon enantioselectivity was examined with **16b** and (*S*)-$\mathbf{12}^+\,PF_6^-$ (entries 9, 6, 10, 11, 12). An inverse dependence was observed, in other words lower *ee* values of **17b** at higher pressures. This has been found for many other rhodium catalysts with chiral chelating diphosphines.[16d, e] The *ee* values also decreased at lower temperature (entries 6, 14, 15). The mechanistic basis for these phenomena has been analyzed in detail.[16c–e] They strongly suggest that our new catalysts exhibit analogous C=C enantioface binding equilibria and reactivity patterns. Turnover frequencies were measured by monitoring hydrogen uptake with a gas burette. Values ranged from 0.028 to 0.083 s^{-1} (100–300 h^{-1}) for (*S*)-$\mathbf{6}^+\,PF_6^-$, and 0.43–0.83 s^{-1} (1550–2970 h^{-1}) for (*S*)-$\mathbf{12}^+\,PF_6^-$. Thus, the less selective catalyst is more reactive. Complex (*S*)-$\mathbf{6}^+\,PF_6^-$ gave similar yields and turnover frequencies in CH_2Cl_2 and methanol, but enantioselectivities were not assayed.

The yields and catalyst loadings (0.5 mol%) in Table 5 translate to turnover numbers of 140–195. We sought to probe the efficacy of lower loadings. Accordingly, the reaction in entry 6 was repeated in a more concentrated solution with 0.05 mol% catalyst. Hydrogen was taken up over the course of 1.5 h (TOF 0.50 s^{-1} or 1800 h^{-1}). Workup gave **17b** in 81% yield (70% *ee*), corresponding to a turnover number of 1620. However, considering the spectroscopically quantitative nature of these reactions, we believe that the true value is closer to 2000. Regardless, (*S*)-$\mathbf{6}^+\,PF_6^-$ and (*S*)-$\mathbf{12}^+\,PF_6^-$ may be used at very low loadings.

0947-6539/01/0709-2022 $ 17.50+.50/0 *Chem. Eur. J.* **2001**, *7*, No. 9

Discussion

Schemes 2 and 3 document the ready availability of a novel new class of chiral chelating diphosphines [(*R*)-**5**, (*S*)-**11**], which, due to the presence of a chiral transition metal in the backbone, present heretofore inaccessible types of steric and electronic environments. These give rhodium adducts that are enantioselective hydrogenation catalyst precursors and show very promising first-generation effectiveness, approaching some the best performance benchmarks in the literature. There is no reason to doubt that optimization of this catalyst class would not match or exceed these benchmarks. Therefore, we focus the first part of this discussion on comparisons with ferrocene-based chiral chelating diphosphines (**A**, **A′**; Scheme 1). A logical starting question is "how easily can each type of chelating diphosphine be synthesized?"

The conversion of commercially available $Re_2(CO)_{10}$ to the non-racemic methyl complex (*S*)-**1** and then diphosphines (*R*)-**5** or (*S*)-**11** requires eleven steps (including two tandem steps, such as the BuLi/PPh_2Cl sequences). The overall yields are 30% and 32%, respectively. Scheme 5 summarizes analogous statistics for three representative ferrocene-based phosphines, **18**–**20**.[4b, 37b] These require seven-fifteen steps from ferrocene, with 15–40% overall yields. Thus, our chelates compare favorably from a preparative standpoint. Our starting material is more expensive than ferrocene, but this becomes less of a factor over a multistep sequence. Furthermore, both enantiomeric series of rhenium complexes are equally available.[19]

Another important comparison involves hydrogenation enantioselectivities. The best of the dozens of rhodium catalysts derived from ligand types **A**/**A′** deliver **17a**–**c** in 97–99% *ee*,[37b, 38] as compared to 88–93% *ee* with (*S*)-**6**$^+$ PF_6^-. Of course, other types of chiral chelating diphosphines give similar or still higher values. From this extensive literature, we emphasize the DuPHOS ligand family.[16a,b] Here, care was also taken to document TON values, which for preparative reactions (>10 g) were routinely 10000. This is larger than the maximum we have demonstrated (1620), but we are confident our catalysts would match it on similar time and mass scales. Thus, although an about 10% improvement in *ee* values is needed to render our catalyst family competitive, there are no identifiable drawbacks or disadvantages associated with the rhenium in the chelate backbone.

In addition, the rhenium-containing chelating diphosphines have many intrinsic diversity elements. All three phosphorus centers are easily modified.[39] The corresponding pentamethylcyclopentadienyl complexes are also available in enantiomerically pure form,[40] and tetra- or trisubstituted homologues should be similarly accessible. It would be easy to replace the methylene group in the larger chelating ligand **11** by either configuration of a CHR stereocenter.[29c] There are also many ways by which **1** could be elaborated on a solid support, or that mixed phosphorus/nitrogen or phosphorus/sulfur donors could be accessed.

Some related heterobimetallic complexes that have been prepared by other groups deserve emphasis. Brunner has reported the chiral molybdenum–rhodium complex **21**, which is shown in Scheme 6 and features molybdenum, carbon, and nitrogen stereocenters. It catalyzed the hydrosilylation of ketones, but only modest *ee* values were obtained.[8a] Moïse has synthesized novel chiral tantalum complexes with diphenylphosphido and diphenylphosphidocyclopentadienyl ligands.[41] He has shown that these can chelate to other metals, as illustrated by **22** in Scheme 6. However, only racemic

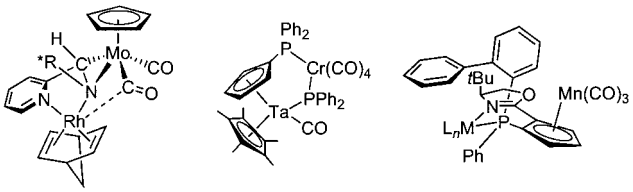

21 **22** **23**

Scheme 6. Other relevant literature compounds.

complexes have been described to date. Finally, the mixed phosphorus/nitrogen donor ligand **23** has been reported by Helmchen.[42] It features a cyclopentadienyl $Mn(CO)_3$ moiety with planar chirality, and other stereogenic elements. Many would have feared that the manganese would be too labile for most types of catalytic reactions. Nonetheless, this ligand is extremely effective for palladium-catalyzed enantioselective allylic substitutions.

In conclusion, this study has established the ready availability and efficacy of a new and architecturally novel type of chiral chelating diphosphines for metal-catalyzed enantioselective organic reactions. The general strategy, exemplified by **B** in Scheme 1, can easily be extended to a broad new family of chelates. By every criterion, these appear capable of impacting catalysis analogously to ferrocene-based chiral chelates of the types **A** and **A′**. Additional types of catalyst precursors and applications will be reported in the near future.[17]

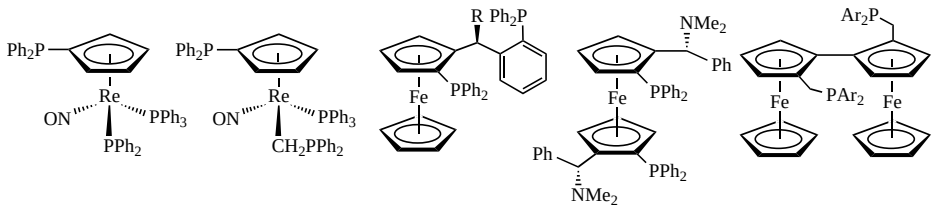

(*R*)-**5**	(*S*)-**11**	**18**	**19**	**20**
10 steps from $Re_2(CO)_{10}$, 30% overall	10 steps from $Re_2(CO)_{10}$, 32% overall	7-8 steps from ferrocene,[37a] 15-35% overall	7 steps from ferrocene,[37b] 40% overall	15 steps from ferrocene,[4b] 25-35% overall

Scheme 5. Comparison of syntheses of representative "metal-containing" chelating diphosphines.

Experimental Section

General data: All reactions except hydrogenations were carried out under dry N_2 atmospheres with glassware that had been oven-dried (100°C), assembled while warm, and cooled under vacuum. New compounds were characterized as follows: IR and NMR

spectra, standard FT instruments; optical rotations, Perkin–Elmer 241 spectropolarimeter; ORD/CD spectra, JASCO J-20C spectrophotometer; mass spectra, VG 770 or Micromass Zabspec instruments; microanalyses, Schwarzkopf Laboratories or in-house service (Carlo Erba EA 1110). Chromatography was conducted with standard instruments under conditions detailed below.

Solvents were treated as follows and stored under N_2: CH_2Cl_2 and $CHCl_3$, distilled from Sicapent (Fluka); benzene, distilled from CaH_2; THF, diethyl ether, and toluene, distilled from Na/O=CPh_2; pentane and hexane, distilled from Na; methanol and ethanol, distilled from Mg; chlorobenzene (Fluka, >99.5%), stored over molecular sieves; CD_2Cl_2 and $CDCl_3$, trap-to-trap distilled from molecular sieves; C_6D_6 and D_8[THF], trap-to-trap distilled from Na/Pb alloy. Reagents were treated as follows: $[Rh(NBD)Cl]_2$ (Strem, >99%), used as received; PPh_2H (>95%), $AgPF_6$ (>99%), and $Ph_3C^+BF_4^-$ (Fluka), used as received; PPh_2Cl (Fluka, ≈97%), freshly vacuum distilled; *n*BuLi (Fluka, ≈1.6 M in hexanes) and *t*BuLi (Fluka, ≈1.5 M in pentane), standardized;[43] hydrogenation substrates, used as received (**16a**,**b**; Fluka) or prepared by standard procedures (**16c**,**d**);[44] others, used as received from common commercial sources.

(*S*)-[(η^5-C_5H_5)Re(NO)(PPh_3)(PPh_2H)]$^+$ BF_4^- [(*S*)-2**$^+$ BF_4^-]:**[19] A Schlenk flask was charged with (*R*)-[(η^5-C_5H_5)Re(NO)(PPh_3)(CH_3)], [(*R*)-**1**],[9] (0.833 g, 1.49 mmol) and chlorobenzene (150 mL), and cooled to −41 °C (CH_3CN/CO_2). Then HBF_4 (5.5 M in diethyl ether; 0.271 mL, 1.5 mmol) was added with stirring. After 10 min, PPh_2H (0.416 g, 2.24 mmol) was added to the dark red solution. The cold bath was allowed to warm. After 12 h, the mixture was slowly added to diethyl ether (400 mL). The tan powder was isolated by filtration, washed with pentane (300 mL) and dried by oil pump vacuum to give (*S*)-**2**$^+$ BF_4^- (1.078 g, 1.320 mmol, 89%). M.p. 210–215 °C decomp; elemental analysis calcd (%) for $C_{35}H_{31}BF_4NOP_2Re$ (816.6) for: C 51.48, H 3.83; found: C 51.59, H 3.96; $[\alpha]_{589}^{22} = -87°$ ($c = 0.11$ mg mL^{-1}, CH_2Cl_2); ^{1}H NMR (300 MHz, CD_2Cl_2, 25 °C, TMS): $\delta = 7.60-7.04$ (m, 5 C_6H_5), 7.34 (dd, ^1J(H,P) = 392 Hz, ^3J(H,P) = 5.4 Hz, PH), 5.33 (s, C_5H_5); ^{31}P{^{1}H} NMR (121 MHz, CD_2Cl_2, 25 °C, H_3PO_4): $\delta = 13.3$ (d, ^2J(P,P) = 13 Hz, PPh_3), −5.5 (d, ^2J(P,P) = 13 Hz, PPh_2H). The ^{13}C NMR spectrum was similar to that of (*S*)-**2**$^+$ OTs^-.[13a]

(*S*)-[(η^5-C_5H_5)Re(NO)(PPh_3)(PPh_2)] [(*S*)-3]:[19] This compound was prepared from (*S*)-**2**$^+$ BF_4^- in 89–96% yields by a deprotonation analogous to that used to synthesize racemic **3** from **2**$^+$ OTs^-.[13a] M.p. 220–230 °C decomp; $[\alpha]_{589}^{22} = 205°$ ($c = 1.05$ mg mL^{-1}, THF).

[(η^5-$C_5H_4PPh_2$)Re(NO)(PPh_3)(H)] (14)

A) A Schlenk flask was charged with PPh_2H (0.13 mL, 0.14 g, 0.75 mmol) and THF (5 mL), and fitted with a septum. Then *n*BuLi (1.40 M in hexane; 0.580 mL, 0.790 mmol) was added with stirring. The colorless solution turned orange. A ^{31}P NMR spectrum of an aliquot showed the clean formation of $LiPPh_2$ ($\delta = -29.90$, s). The solution was transferred by cannula with stirring to a septum-capped Schlenk tube that had been charged with [(η^5-C_5H_5)Re(NO)(PPh_3)(OTs)] (**13**;[30] 0.50 g, 0.70 mmol) and THF (20 mL). The red solution was stirred and gradually turned yellow. A ^{31}P NMR spectrum of an aliquot showed complete product formation. After 4 h, the volatiles were removed by oil-pump vacuum. The yellow residue was extracted with benzene. The extract was filtered through a Celite plug. The bright yellow filtrate was concentrated, and hexanes added by vapor diffusion. Yellow needles slowly formed, which were collected by filtration and dried by oil pump vacuum to give **14** (0.43 g, 0.60 mmol, 85%). M.p. 198–200 °C decomp; elemental analysis calcd (%) for $C_{35}H_{30}NOP_2Re$ for: C 57.68, H 4.15, P 8.50; found: C 57.62, H 4.35, P 8.34; IR (KBr, cm^{-1}): $\tilde{\nu} = 1950$ (s, ReH), 1633 (s, NO); ^{1}H NMR (300 MHz, CD_2Cl_2, 28 °C, TMS): $\delta = 7.50-7.31$ (br m, 5 C_6H_5), 4.91, 4.87, 4.65, 4.58 (4 br m, C_5H_4), −9.56 (dd, ^2J(H,P) = 29.7 Hz, ^3J(H,P) = 1.8 Hz, ReH); ^{13}C{^{1}H} NMR (75 MHz, CD_2Cl_2, 28 °C, TMS): PPh_3 at $\delta = 138.2$ (d, ^1J(C,P) = 53 Hz, i), 134.0 (d, ^2J(C,P) = 11 Hz, o), 129.0 (s, p); PPh_2 at 138.7 (d, ^1J(C,P) = 57 Hz, i), 138.5 (d, ^1J(C,P) = 56 Hz, i′), 133.7 (d, ^2J(C,P) = 9 Hz, o), 130.4 (s, p); other PPh_3, PPh_2 at 128.7–128.5 (m); C_5H_4 at 94.9 (d, ^1J(C,P) = 14 Hz, CP), 93.3 (s), 89.9 (d, ^2J(C,P) = 10 Hz), 88.9 (s), 88.7 (s); ^{31}P{^{1}H} NMR (121 MHz, CD_2Cl_2, 25 °C, H_3PO_4): $\delta = 26.1$ (s, PPh_3), −14.9 (s, $C_5H_4PPh_2$).

B)[19] An analogous synthesis was conducted with (*S*)-**13** (0.200 g, 0.280 mmol).[30] A similar workup gave yellow needles of (*R*)-**14** (0.160 g, 0.220 mmol, 79%). The IR and NMR (^{1}H, ^{13}C, ^{31}P) spectra were similar to those of the racemate. $[\alpha]_{589}^{22} = -89°$ ($c = 1.0$ mg mL^{-1}, THF). See text for comments on the enantiomeric purity and configurational assignment.

[(η^5-$C_5H_4PPh_2$)Re(NO)(PPh_3)(PPh_2)] (5)

A) A Schlenk tube was charged with **14** (0.100 g, 0.140 mmol)[13a] and THF (10 mL), capped with a septum, and cooled to −15 °C (ethylene glycol/CO_2). Then *n*BuLi (1.4 M in hexane; 0.011 mL, 0.15 mmol) was added with stirring. The light yellow solution turned deep red. After 20 min, the tube was transferred to a −78 °C bath (acetone/N_2). Then PPh_2Cl (0.027 mL, 0.033 g, 0.15 mmol) was added dropwise with stirring, giving an orange solution. The cold bath was allowed to warm. After 4–6 h, the volatiles were removed by oil-pump vacuum. The residue was extracted with benzene. The extract was filtered through a Celite plug. The filtrate was concentrated, and hexanes were added by vapor diffusion. Red flower-like crystals slowly formed, which were collected by filtration and dried (10^{-3} Torr, 56 °C, 12 h) to give **5**·$(C_6H_6)_{0.5}$ (0.089 g, 0.093 mmol, 68%). M.p. 196–197 °C decomp; elemental analysis calcd (%) for: $C_{47}H_{39}NOP_3Re \cdot (C_6H_6)_{0.5}$ (952.0): C 63.08, H 4.45, P 9.76; found: C 63.52, H 4.58, P 9.02; IR (KBr, cm^{-1}): $\tilde{\nu} = 1656$ (s, NO); ^{1}H NMR (300 MHz, [D_8]THF, 28 °C, TMS): $\delta = 7.47-7.27$, 7.16–6.92 (2 m, 7 C_6H_5), 7.26 (br s, 0.5 C_6H_6), 5.34, 5.12, 4.59, 3.02 (4 br s, C_5H_4); ^{13}C{^{1}H} NMR (75 MHz, [D_8]THF, 28 °C, TMS): PPh_3 and PPh_2 at $\delta = 139.2$ (d, ^2J(C,P) = 11 Hz, o), 136.7 (d, ^2J(C,P) = 11 Hz, o′), 136.1 (d, ^1J(C,P) = 54 Hz, i), 135.2–133.9, 130.8–126.0 (2 br m, Ph); 129.0 (s, C_6H_6); C_5H_4 at 101.4 (d, ^1J(C,P) = 18 Hz, CP), 93.8 (d, J(C,P) = 2 Hz), 91.2 (d, J(C,P) = 3 Hz), 91.2 (s), 90.9 (s); ^{31}P{^{1}H} NMR (121 MHz, [D_8]THF, 28 °C, H_3PO_4): $\delta = 20.2$ (d, ^2J(P,P) = 15 Hz, PPh_3), −16.2 (s, $C_5H_4PPh_2$), −45.2 (d, ^2J(P,P) = 15 Hz, $RePPh_2$).

B)[19] A Schlenk tube was charged with (*S*)-**3** (0.500 g, 0.620 mmol) and THF (30 mL), capped with a septum, and cooled to −78 °C. Then *n*BuLi (1.6 M in hexanes, 0.43 mL, 0.69 mmol) was slowly added with stirring. After 15 min, an aliquot was assayed by ^{31}P NMR (Table 1; complete formation of (*S*)-**4**). Then PPh_2Cl was added (0.110 mL, 0.140 g, 0.620 mmol; caution: any excess can react with the product). The mixture was stirred for 30 min at −78 °C, and the cold bath was allowed to warm. After 4–6 h, the volatiles were removed by rotary evaporation. The red foam was dried (10^{-3} Torr, 6 h) to give (*S*)-**5** (0.520 g, 0.550 mmol, 89%), which was pure by NMR. A portion (0.035 g, 0.037 mmol) was dissolved in benzene, and hexanes were added by vapor diffusion. Red prisms slowly formed, which were collected by filtration and dried as above to give (*S*)-**5**·$(C_6H_6)_{0.5}$ (0.020 g, 0.021 mmol, 60%).[19] The IR and NMR (^{1}H, ^{13}C, ^{31}P) spectra were similar to those of the racemate. $[\alpha]_{589}^{22} = 216°$ ($c = 1.0$ mg mL^{-1}, THF).

[(η^5-$C_5H_4PPh_2$)Re(NO)(PPh_3)(μ-PPh_2)Rh(NBD)]$^+$ PF_6^- [(6$^+$ PF_6^-)]

A) A Schlenk flask was charged with **5**·$(C_6H_6)_{0.5}$ (0.505 g, 0.533 mmol) and THF (25 mL), and $[Rh(NBD)Cl]_2$ (0.12 g, 0.26 mmol) was added with stirring. The orange solution turned deep red, and $AgPF_6$ (0.155 g, 0.582 mmol) was added. The sample became heterogeneous and red-brown. After 30 min, the volatiles were removed in vacuo. The residue was extracted with benzene. The extract was filtered through a Celite plug. The deep red filtrate was concentrated, and hexanes were added. The dark orange solid was dissolved in a minimum of THF, and pentane was added by vapor diffusion at −20 °C. Orange-red, plate-like crystals slowly formed, which were collected by filtration and dried (10^{-3} Torr, 24 h) to give **6**$^+$ PF_6^-·THF (0.605 g, 0.445 mmol, 83%). M.p. 180–183 °C decomp; elemental analysis (%) calcd for $C_{54}H_{47}F_6NOP_4ReRh \cdot C_4H_8O$ (1325.1): C 52.57, H 4.48, P 9.35; found: C 52.53, H 4.52, P 9.34; IR (KBr, cm^{-1}): $\tilde{\nu} =$ 1670 (s, NO); MS (FAB, 3-NBA): m/z (%): 1108 (58) [M]$^+$, 600 (50), 183 (74), 154 (100); ^{1}H NMR (300 MHz, CD_2Cl_2, 28 °C, TMS): $\delta = 8.10-8.04$, 7.70–7.65, 7.51–7.43, 7.36–7.31, 7.29–7.23, 7.23–7.08, 6.71–6.64 (7 m, 7 C_6H_5), 5.69, 5.51, 5.45, 4.66, 4.52, 4.45, 4.01, 4.00, 3.79, 3.69 (10 br s, C_5H_4, NBD CH), 3.69–3.65, 1.84–1.79 (2 m, THF), 1.56 (dd, ^2J(H,H′) = 8.9 Hz, ^3J(H,H″) = 1.6 Hz, NBD-C*H*H′), 1.44 (dd, ^2J(H′,H) = 8.5 Hz, ^3J(H′,H″) = 1.5 Hz, NBD-CH*H*′); ^{13}C{^{1}H} NMR (75 MHz, CD_2Cl_2, 28 °C, TMS): PPh_3, PPh_2 at $\delta = 142.0$ (d, ^1J(C,P) = 20 Hz, i), 134.2 (d, ^1J(C,P) = 54 Hz, i′), 137.3 (d, ^1J(C,P) = 20 Hz, i″), 136.2 (d, J(C,P) = 14 Hz), 134.8 (d, J(C,P) = 13 Hz), 133.6 (s), 133.6 (d, J(C,P) = 11 Hz), 131.8 (d, J(C,P) = 11 Hz), 131.2–130.9 (m), 130.1–128.8 (m); C_5H_4, NBD at 114.6 (s), 114.5 (s), 110.8 (s), 110.2 (s), 102.5 (d, ^1J(C,P) = 18 Hz, CP), 98 (s), 96.1 (br m), 89.1 (br m), 83.2 (s), 81.7 (br m), 71.8 (br m), 69.9 (s); 68.2, 26.0 (2 s, THF); ^{31}P{^{1}H} NMR (121 MHz, CD_2Cl_2, 28 °C, H_3PO_4): $\delta = 50.4$ (ddd, ^1J(P,Rh) = 183 Hz, ^2J(P,P) = 19 Hz, ^3J(P,P) = 5 Hz, $C_5H_4PPh_2$), 9.8 (dd, ^2J(P,P) = 14 Hz,

0947-6539/01/0709-2024 $ 17.50+.50/0 *Chem. Eur. J.* **2001**, *7*, No. 9

^3J(P,P) = 5 Hz, PPh_3), −49.2 (ddd, ^1J(P,Rh) = 127 Hz, ^2J(P,P) = 19 Hz, ^2J(P,P) = 14 Hz, $RePPh_2$), −144.0 (sep, ^1J(P,F) = 708 Hz, PF_6).

B) A sample was dissolved in $CHCl_3$ and layered with hexanes. Dark red prisms of **6**$^+$ $PF_6^-\cdot(CHCl_3)_2$ formed, and were used for crystallography (below). The solvate was verified by ^{13}C NMR.

C)[19] The compounds (*S*)-**5**$\cdot(C_6H_6)_{0.5}$ (0.185 g. 0.192 mmol), THF (15 mL), $[Rh(NBD)Cl]_2$ (0.046 g, 0.096 mmol), and $AgPF_6$ (0.50 g, 0.200 mmol) were combined as in procedure A. After 2 h, the volatiles were removed in vacuo. The residue was extracted with benzene. The extract was filtered through a Celite plug. The solvent was removed from the filtrate by rotary evaporation. The residue was dried (10^{-3} Torr, 6 h) to give (*R*)-**6**$^+$ $PF_6^-\cdot$ THF (0.24 g, 0.18 mmol, 92 %)[19] as a dark orange powder that was pure by NMR (^1H, ^{13}C, ^{31}P; data similar to racemate). Crystallization attempts gave oils. $[\alpha]_{589}^{22} = 48^\circ$ ($c = 1.0$ mg mL^{-1}, THF).

[(η^5-C_5H_5)Re(NO)(PPh_3)(CH_2PPh_2H)]$^+$ BF_4^- [8**$^+$ BF_4^-]**

A) A Schlenk flask was charged with **1** (1.000 g, 1.790 mmol) and CH_2Cl_2 (50 mL), and was cooled to −60 °C (acetone/N_2 slurry). Then $Ph_3C^+BF_4^-$ (0.650 g, 1.97 mmol, 1.1 equiv) was added with stirring. Within 30 min, the orange suspension turned to a light green-yellow solution. Then PPh_2H (0.0168 mL, 0.180 g, 0.967 mmol, 1.2 equiv) was added dropwise with stirring. After 10 min, the cold bath was removed. The solution turned orange and then red. After 1.5 h, the mixture was concentrated to about 15 mL by a brief exposure to oil pump vacuum. Some product crystallized. The sample was layered with hexanes (40 mL). After 24 h, the orange-red prisms were collected by filtration, washed with hexanes (2 × 5 mL), and dried (10^{-3} Torr, 1 h) to give **8**$^+$ $BF_4^-\cdot CH_2Cl_2$ (1.560 g, 1.704 mmol, 95 %). M.p. 202–206 °C; elemental analysis (%) calcd for $C_{36}H_{33}BF_4NOP_2Re\cdot CH_2Cl_2$ (915.6): C 48.54, H 3.85, N 1.53; found: C 48.65, H 3.87, N 1.54; IR (KBr, cm^{-1}): $\tilde{\nu}$ = 1662 (s, NO); MS (FAB, 3-NBA): *m*/*z* (%): 744 (87) $[M]^+$, 558 (100) $[M - HPPh_2]^+$, 481 (24) $[M - PPh_3]^+$; ^1H NMR (400 MHz, CD_2Cl_2, 28 °C, TMS): δ = 7.86–7.25 (m, 5 C_6H_5), 7.18 (ddd, ^1J(H,P) = 489 Hz, ^3J(H,H) = 11.0 Hz, ^3J(H,H′) = 5.1 Hz, HP), 5.32 (s, CH_2Cl_2), 4.95 (s, C_5H_5), 2.58–2.44 (m, CHH′); $^{13}C\{^1H\}$ NMR (100.5 MHz, CD_2Cl_2, 28 °C, TMS): PPh_3 at δ = 134.3 (d, ^1J(C,P) = 55 Hz, i), 133.9 (d, ^2J(C,P) = 11 Hz, o), 131.4 (s, p), 129.3 (d, ^3J(C,P) = 9 Hz, m); PPhPh′ at 134.5 (s, p), 132.5 (d, ^2J(C,P) = 9 Hz, o), 132.0 (d, ^2J(C,P) = 9 Hz, o′), 130.3 (d, ^3J(C,P) = 11 Hz, m), 130.1 (d, ^3J(C,P) = 11 Hz, m′), 124.7 (d, ^1J(C,P) = 72 Hz, i), 123.3 (d, ^1J(C,P) = 85 Hz, i′); 91.0 (s, C_5H_5), −35.4 (d, ^1J(C,P) = 29 Hz, CH_2); $^{31}P\{^1H\}$ and ^{31}P NMR (161.7 MHz, CD_2Cl_2, 28 °C, H_3PO_4): δ = 21.7 (d, ^3J(P,P) = 12 Hz) or 21.7 (br s, $w_{1/2}$ = 38 Hz) (PPh_3), 30.2 (d, ^3J(P,P) = 12 Hz) or 30.2 (d, ^1J(H,P) = 487 Hz, each line with $\nu_{1/2}$ = 42 Hz) (PPh_2).

B) An analogous synthesis was conducted with (*S*)-**1** (1.000 g, 1.790 mmol).[9] The CH_2Cl_2 solution (15 mL) was layered with pentane (40 mL). After 1 d, red prisms were collected by filtration, washed with pentane (2 × 5 mL), and dried by oil pump vacuum to give (*S*)-**8**$^+$ BF_4^- (1.460 g, 1.758 mmol, 98 %). M.p. 192–196 °C; elemental analysis (%) calcd for $C_{36}H_{33}BF_4NOP_2Re$ (830.6): C 52.06, H, 4.00, N 1.69; found: C 52.02, H 4.08, N 1.55; $[\alpha]_{589}^{24} = 175^\circ$ ($c = 1.68$ mg mL^{-1}, $CHCl_3$). The NMR spectra (^1H, ^{13}C, ^{31}P) were similar to those of the racemate.

[(η^5-C_5H_5)Re(NO)(PPh_3)(CH_2PPh_2)] (9)

A) A Schlenk tube was charged with **8**$^+$ $BF_4^-\cdot CH_2Cl_2$ (1.554 g, 1.697 mmol) and THF (60 mL). A solution of *t*BuOK (1.0 M in THF; 2.43 mL, 2.43 mmol) was added with stirring. After 1 h, the solvent was removed by oil pump vacuum. Benzene (20 mL) was added, and the sample was filtered through a Celite plug (4 × 2 cm). The filtrate was concentrated (to ca. 10 mL) and layered with pentane (30 mL). After 24 h, the supernatant was decanted from orange-red needles, which were dried by oil pump vacuum to give **9** (1.250 g, 1.548 mmol, 90 %). M.p. 178–179 °C decomp; elemental analysis (%) calcd for $C_{36}H_{32}NOP_2Re$ (742.8): C 58.21, H 4.34, N 1.89; found: C 58.32, H 4.25, N 1.68; IR (KBr, cm^{-1}): $\tilde{\nu}$ = 3051 (m, CH), 1638 (s, NO); MS (FAB, 3-NBA): *m*/*z* (%): 742 (40) $[M]^+$, 558 (100) $[MH - PPh_2]^+$, 481 (66) $[M - PPh_3]^+$; ^1H NMR (400 MHz, $CDCl_3$, 28 °C, TMS): δ = 7.62–7.16 (m, 5 C_6H_5), 4.86 (s, C_5H_5), 2.49 (dd, J(H,P) = 9.9 Hz, ^2J(H,H′) = 12.1 Hz, C*H*H′), 1.84 (dd, J(H′,P) = 2.0 Hz, ^2J(H′,H) = 12.1 Hz, CH*H*′); $^{13}C\{^1H\}$ NMR (100.4 MHz, $CDCl_3$, 28 °C, TMS): PPh_3 at δ = 135.8 (d, ^1J(C,P) = 53 Hz, i), 133.6 (d, ^2J(C,P) = 11 Hz, o), 130.1 (s, p), 128.4 (d, ^3J(C,P) = 9 Hz, m); PPhPh′ at 146.6 (d, ^1J(C,P) = 20 Hz, i), 145.3 (d, ^1J(C,P) = 18 Hz, i′), 133.0 (d, ^2J(C,P) = 18 Hz, o), 132.7 (d, ^2J(C,P) = 17 Hz, o′), 127.7 (d, ^3J(C,P) = 7 Hz, m), 127.6 (d, ^3J(C,P) = 6 Hz, m′), 127.4 (s, p), 127.0 (s, p′); 89.8 (s, C_5H_5), −19.5 (d, ^1J(C,P) = 35 Hz, CH_2); $^{31}P\{^1H\}$ and ^{31}P NMR (161.7 MHz, $CDCl_3$, 28 °C, H_3PO_4): δ = 8.1 (d, ^3J(P,P) = 8 Hz) or 8.1 (dd, ^3J(P,P) = 6 Hz, ^2J(H,P) = 12.1 Hz) (PPh_2), 25.8 (d, ^3J(P,P) = 8 Hz, PPh_3) or 25.7 (br s, PPh_3).

B) An analogous synthesis was conducted with (*S*)-**8**$^+$ BF_4^- (1.420 g, 1.710 mmol). Workup gave (*S*)-**9**$\cdot C_6H_6$ as orange needles (1.246 g, 1.518 mmol, 89 %). M.p. 172 °C decomp; $[\alpha]_{589}^{24} = 220^\circ$ ($c = 2.70$ mg mL^{-1}, THF); elemental analysis (%) calcd for $C_{36}H_{32}NOP_2Re\cdot C_6H_6$ (820.9): C 61.45, H 4.67, N 1.71; found: C 61.15, H 4.68, N 1.71. The NMR spectra (^1H, ^{13}C, ^{31}P) were similar to those of the racemate. The crystallization supernatant was kept at room temperature for several hours. Clear orange cubes (0.2–1.0 mm edges) of (*S*)-**9**$\cdot C_6H_6$ formed. One was removed for a crystal structure (below). The supernatant was decanted. The remaining cubes were dried under a N_2 stream (0.065 g, 0.079 mmol, 5 %). Elemental analysis (%) found: C 61.86, H 4.66, N 1.75 (calcd, see above).

[(η^5-$C_5H_4PPh_2$)Re(NO)(PPh_3)(CH_2PPh_2)] (11)

A) A Schlenk tube was charged with **9** (1.210 g, 1.629 mmol) and THF (60 mL), and was cooled to −60 °C (acetone/N_2 slurry). A solution of *t*BuLi (1.5 M in pentane; 1.30 mL, 1.96 mmol, 1.2 equiv) was slowly added against a N_2 flow with stirring. The cold bath was replaced by a 0 °C ice bath. The orange mixture turned orange-red. An aliquot was assayed by ^{31}P NMR (Table 1; complete formation of **10**). After 30 min, PPh_2Cl (0.331 mL, 0.395 g, 1.792 mmol) was added. The bath was allowed to warm to room temperature over the course of 1 h. The solvent was removed by oil-pump vacuum. Benzene (20 mL) was added. The mixture was filtered through a Celite plug (2 × 6 cm; with benzene rinses). The filtrate was concentrated to 10 mL. A pentane layer (30 mL) was gently added. After 2 d, the supernatant was decanted from a mixture of bright red crystals and yellow powder to give **11** (1.024 g, 1.105 mmol, 68 %). M.p. 115–118 °C decomp; elemental analysis (%) calcd for $C_{48}H_{41}NOP_3Re$ (927.0): C 62.19, H 4.46, N 1.51; found: C 62.02, H 4.81, N 1.14; IR (KBr, cm^{-1}): $\tilde{\nu}$ = 3051, 2907, 2868 (w, CH), 1637 (s, NO); MS (FAB, 3-NBA): *m*/*z* (%): 926 (38) $[M]^+$, 742 (90) $[M - PPh_2]^+$, 727 (35) $[M - CH_2PPh_2]^+$, 681 (100) $[M - OPPh_3]^+$, 665 (50) $[M - PPh_3]^+$; ^1H NMR (400 MHz, $[D_8]$THF, 28 °C, TMS): δ = 7.56–7.02 (m, 7 C_6H_5), 5.22, 4.82, 4.70, 3.39 (4 br s, C_5H_4), 2.41 (dd, ^2J(H,H′) = 11.8 Hz, J(H,P) = 9.6 Hz, C*H*H′), 1.88 (dd, ^2J(H′,H) = 11.8 Hz, J(H′,P) = 1.9 Hz, CH*H*′); $^{13}C\{^1H\}$NMR (100.6 MHz, $[D_8]$THF, 28 °C, TMS): PPh_3 at δ = 136.6 (d, ^1J(C,P) = 52 Hz, i), 134.7 (d, ^2J(C,P) = 11 Hz, o), 130.6 (s, p), 129.0 (d, ^3J(C,P) = 13 Hz, m); 2 PPhPh′ at 148.0 (d, ^1J(C,P) = 22 Hz, i), 146.7 (d, ^1J(C,P) = 20 Hz, i′), 139.4 (d, ^1J(C,P) = 13 Hz, i″), 137.7 (d, ^1J(C,P) = 11 Hz, i‴), 134.8 (s, p), 128.0 (s, p′), 134.2 (d, ^2J(C,P) = 20 Hz, o), 133.6 (d, ^2J(C,P) = 18 Hz, o′), 133.5 (d, ^2J(C,P) = 15 Hz, o″), 129.5 (d, ^2J(C,P) = 15 Hz, o‴), 129.1 (d, ^3J(C,P) = 4 Hz, m), 128.1 (d, ^3J(C,P) = 4 Hz, m′), 127.4 (d, ^3J(C,P) = 7 Hz, m″); C_5H_4 at 105.5 (br s), 98 (d, J(C,P) = 17 Hz), 91.8 (d, J(C,P) = 4 Hz), 91.2 (s), 89.1 (d, J(C,P) = 18 Hz, CP); −18.2 (d, ^1J(C,P) = 37 Hz, CH_2); $^{31}P\{^1H\}$NMR (161.7 MHz, $[D_8]$THF/C_6D_6, 28 °C, H_3PO_4): δ = 26.3/26.3 (d, ^3J(P,P) = 5/8 Hz, PPh_3), 7.3/6.9 (dd, ^3J(P,P) = 5/3, 5/8 Hz, $C_5H_4PPh_2$), −17.3/−17.7 (d, ^3J(P,P) = 5/3 Hz, PPh_2).

B) A Schlenk flask was charged with (*S*)-**9**$\cdot C_6H_6$ (0.780 g, 1.050 mmol) and THF (30 mL), and cooled to −30 °C (acetone/N_2 slurry). Then *t*BuLi (1.50 M in pentane, 1.05 mL, 1.58 mmol, 1.5 equiv) and PPh_2Cl (0.272 mL, 0.324 g, 1.47 mmol, 1.4 equiv) were added as in procedure A. After 1 h, the solvent was removed by oil pump vacuum. Benzene was added (10 mL). The mixture was filtered through a Celite plug. The filtrate was concentrated to 5 mL. A pentane layer (10 mL) was gently added. After 2 d, the supernatant was decanted. The residue was washed with pentane and dried by oil pump vacuum. The supernatant was evaporated to dryness and the precipitation repeated. The two crops were combined to give (*S*)-**11** as a orange powder (0.677 g, 0.730 mmol, 70 %). Elemental analysis (%) calcd for $C_{48}H_{41}NOP_3Re$ (927.0): C 62.19, H 4.46, N 1.51; found: C 61.73, H 4.60, N 1.41; $[\alpha]_{589}^{24} = 130^\circ$ ($c = 2.80$ mg mL^{-1}, THF). The NMR spectra (^1H, ^{13}C, ^{31}P) were similar to those of the racemate.

[(η^5-$C_5H_4PPh_2$)Re(NO)(PPh_3)(μ-CH_2PPh_2)Rh(NBD)]$^+$ PF_6^- (12$^+$ PF_6^-)

A) A Schlenk tube was charged with **11** (1.024 g, 1.105 mmol) and THF (100 mL), and $[Rh(NBD)Cl]_2$ (0.255 g, 0.552 mmol) was added with stirring. After 30 min, $AgPF_6$ (0.279 g, 1.105 mmol) was added. The sample became heterogeneous and deep brown. After 2 h, the volatiles were removed by oil pump vacuum. Benzene (60 mL) was added, and the mixture was filtered through a Celite plug (3 × 5 cm). The solvent was removed from the filtrate by rotary evaporation. The residue was dried by oil pump vacuum to give crude **12**$^+$ PF_6^- (1.330 g, 1.050 mmol, 95 %) as a

reddish brown solid. A sample (0.110 g, 0.087 mmol) was dissolved in THF (10 mL). The solution was concentrated to ca. 5 mL, and pentane (15 mL) was added. The solid was collected on a frit, washed with small amounts of pentane, and dried by oil pump vacuum to give **12**$^+$ PF_6^- as a light brown powder that was pure by NMR (0.065 g, 0.051 mmol, 59%). M.p. 180–185 °C decomp; elemental analysis (%) calcd for $C_{55}H_{49}F_6NOP_4ReRh$ (1267.0): C 52.14, H 3.90, N 1.11; found: C 51.72, H 4.31, N 0.83; IR (KBr, cm^{-1}): $\tilde{\nu}$ = 3056, 2924 (w, CH), 1663 (s, NO), 1481 (m), 1435 (m), 1309 (w), 1261 (w), 1186 (w), 1160 (w), 1094 (m), 1027 (w), 999 (w), 839 (s, PF), 744 (m), 696 (m); MS (FAB, 3-NBA): *m*/*z* (%): 1122 (100) $[M]^+$, 1030 (40) $[M-NBD]^+$; ^{1}H NMR (400 MHz, $CDCl_3$, 28 °C, TMS): δ = 7.59–7.01 (m, 7 C_6H_5), 5.60, 5.42, 4.86, 4.00 (4 br s, C_5H_4), 4.90, 4.53, 4.43, 4.00, 3.95, 3.72 (6 br s, NBD-CH), 1.42 (br s, NBD-CH_2), 2.25 (m, C*H*H′), 2.07 (m, CH*H*′); ^{13}C{^{1}H} NMR (100.6 MHz, $CDCl_3$, 28 °C, TMS): δ = PPh_3 at 133.1 (d, ^1J(C,P) = 53 Hz, i), 132.5 (d, ^2J(C,P) = 10 Hz, o), 129.8 (d, ^4J(C,P) = 2 Hz, p), 127.8 (d, ^3J(C,P) = 11 Hz, m); 2 RhPPhPh′ at 138.2 (d, ^1J(C,P) = 29 Hz, i), 134.1 (d, ^1J(C,P) = 47 Hz, i′), 134.1 (d, ^2J(C,P) = 11 Hz, o), 133.4 (d, ^2J(C,P) = 13 Hz, o′), 131.7 (d, ^2J(C,P) = 11 Hz, o″), 131.2 (d, ^2J(C,P) = 10 Hz, o‴), 130.1 (d, ^3J(C,P) = 8 Hz, m), 128.4 (d, ^3J(C,P) = 10 Hz, m′), 128.0 (d, ^3J(C,P) = 11 Hz, m″), 127.6 (d, ^3J(C,P) = 7 Hz, m‴) 130.8 (d, ^4J(C,P) = 2 Hz, p), 129.9 (d, ^4J(C,P) = 3 Hz, p′), 129.7 (d, ^4J(C,P) = 2 Hz, p″), 128.3 (d, ^4J(C,P) = 2 Hz, p‴); C_5H_4 and NBD at 97.6 (s), 94.8 (d, ^1J(C,P) = 16 Hz, CP), 93.8 (s), 90.5 (m), 87.9 (m), 85.2 (s), 84.3 (s), 80.2 (s), 69.1 (s), 67.9 (s), 53.7 (s), 52.5 (s); −14.2 (br s, $ReCH_2$); ^{31}P{^{1}H} NMR (161.7 MHz, $CDCl_3$, 28 °C, H_3PO_4): δ = 50.5 (ddd, ^1J(P,Rh) = 148 Hz, ^2J(P,P) = 34 Hz, ^3J(P,P) = 18 Hz, $C_5H_4PPh_2$), 23.9 (ddd, ^1J(Rh,P) = 166 Hz, ^2J(P,P) = 34 Hz, ^3J(P,P) = 4 Hz, CH_2PPh_2), 20.2 (dd, ^3J(P,P) = 18 Hz, ^3J(P,P) = 4 Hz, PPh_3), −156.5 (sep, ^1J(P,F) = 708 Hz, PF_6).

B) A solution of crude **12**$^+$ PF_6^- (0.070 g) in CH_2Cl_2 (5 mL) was layered with hexane (30 mL). After three weeks, deep red prisms of **12**$^+$ $PF_6^-\cdot CH_2Cl_2$ formed. One was removed for a crystal structure (below). The supernatant was decanted, and the remaining prisms were dried under a N_2 stream. Elemental analysis (%) calcd for $C_{56}H_{51}Cl_2F_6NOP_4ReRh$ (1351.9): C 49.75, H 3.80, N 1.04; found: C 49.72, H 3.97, N 0.97.

C) A Schlenk tube was charged with (*S*)-**11** (0.609 g, 0.657 mmol) and THF (50 mL), and $[Rh(NBD)Cl]_2$ (0.151 g, 0.328 mmol) was added with stirring. After 1 h, $AgPF_6$ (0.166 g, 0.657 mmol) was added. After 1 h, the volatiles were removed by oil pump vacuum. Benzene (30 mL) was added. The mixture was filtered through a Celite plug. The solvent was removed from the filtrate by oil pump vacuum. The brown semisolid was dissolved in a minimum of benzene, and pentane was added. The precipitate was collected by filtration, washed with pentane (10 mL) and dried by oil pump vacuum to give (*S*)-**12**$^+$ PF_6^- as a deep brown powder (0.680 g, 0.537 mmol, 82%). This was reprecipitated from benzene/pentane to give a red-brown powder. M.p. 180–185 °C decomp; $[\alpha]_{589}^{24} = -65°$ (c = 0.80 mg mL^{-1}, THF). Both samples showed small amounts of impurities by NMR (<2%), and microanalyses were slightly off. The ^{13}C NMR spectra were similar to that of the racemate, but the ^{1}H and ^{31}P NMR spectra showed minor differences. Hence, these data are given below. ^{1}H NMR (see racemate): δ = 7.62–7.05 (m, 7 C_6H_5), 5.46, 5.42, 4.80, 4.43 (4 br s, C_5H_4), 4.84, 4.58, 4.50, 4.05, 3.96, 3.81 (6 br s, NBD-CH), 1.47 (br s, NBD-CH_2), 2.30 (m, C*H*H′), 2.17 (m, CH*H*′); ^{31}P{^{1}H} NMR (see racemate): δ = 50.7 (ddd, J = 148, 34, 18 Hz, $C_5H_4PPh_2$), 22.6 (ddd, J = 166, 34, 4 Hz, CH_2PPh_2), 19.7 (dd, J = 18, 4 Hz, PPh_3), −158.0 (sep, J = 708 Hz, PF_6).

Hydrogenations (Table 5): A 50 mL flask was charged with **16** (3.00 mmol; typical was entry 6, 0.388 g **16b**), catalyst (0.50 mol%; entry 6: 0.019 g (*S*)-**12**$^+$ PF_6^-), and THF (ca. 25 mL), and attached to a gas burette. The light orange solution was freeze-pump-thaw degassed (4 ×). A H_2 atmosphere was introduced, and the solution vigorously stirred. Within 1 min, H_2 uptake began. After H_2 uptake ceased (entry 6: 58 mL, 2.6 mmol, theory: 67 mL), **17** was isolated by a standard workup (entry 6: 0.338 g per 2.58 mmol **17b**).[27a]

Product configurations were assigned from the signs of optical rotations.[27a, 45] Enantiomeric purities were assayed chromatographically. In one series of determinations,[46] **17a**,**b**,**d** were first treated with methanol/HCl. The resulting methyl esters, and **17c**, were treated with trifluoroacetic anhydride to give *N*-trifluoroacetyl-*N*-acetyl amino esters, which were analyzed by GLC (130 °C, N_2 carrier flow 20 mL min^{-1}, 2 m × 2 mm glass column packed with 5% lauroyl-L-valine-*tert*-butylamide (Supelco SP300) on 100/120 Supelcoport) to give the data communicated earlier[18] and in entries 2–4, Table 5.

In another series of determinations, **17a**,**b** (ca. 0.010 g in 2 mL methanol) were treated with diazomethane/diethyl ether (yellow endpoint) to give methyl esters (solvent was removed under vacuum, the residue was extracted with HPLC grade isopropanol, and the extract filtered through glass wool). The ester from **17a** was analyzed by GLC (100 °C, N_2 carrier flow 20 mL min^{-1}, 25 m × 0.4 mm glass capillary column packed with a modified β-cyclodextrin on silica)[47] to give the data in entries 1 and 5. The ester from **17b**, and esters **17c**,**d**, were analyzed by HPLC (typically 98:2 *v*/*v* isohexane/isopropanol (isocratic), Chiralcel OD with cellulose-carbamate on silica gel) to give the data in entries 6–15.

Crystallography: Data were collected as summarized in Table 2. Cell parameters for **6**$^+$ $PF_6^-\cdot(CHCl_3)_2$ were determined from 15 reflections ($16° < 2\theta < 29°$). Lorentz-polarization corrections were applied. The structure was solved by standard heavy atom techniques (all data by full-matrix-least-squares on F) using the UCLA crystallographic package.[48a] Carbon atoms were refined isotropically, and hydrogen atom positions were calculated. Other atoms were refined anisotropically (Δ/δ (max) = 2.40). Cell parameters for (*S*)-**9**$\cdot C_6H_6$ and **12**$^+$ $PF_6^-\cdot CH_2Cl_2$ were determined from 15 reflections ($5.0° < 2\theta < 50.0°$). Lorentz-polarization and empirical absorption (Ψ scans) corrections were applied. Space groups were determined from systematic absences and subsequent least-squares refinement. The structures were solved by direct methods. The data were refined (all data by full-matrix-least-squares on F^2) using SHELXL-93.[48b] Non-hydrogen atoms were refined with anisotropic thermal parameters. Hydrogen atoms were fixed in idealized positions using a riding model. Scattering factors were taken from literature.[49] The rhenium configuration in (*S*)-**9**$\cdot C_6H_6$ was established by Flack's x parameter (found: −0.006(12); theory for correct and inverted structures: 0 and 1).[50]

Crystallographic data (excluding structure factors) for the structures reported in this paper have been deposited with the Cambridge Crystallographic Data Centre as supplementary publication no. refcode FOWNIO [**6**$^+$ $PF_6^-\cdot(CHCl_3)_2$], CCDC-147776 [(*S*)-**9**$\cdot C_6H_6$] and -147777 [**12**$^+$ $PF_6^-\cdot CH_2Cl_2$]. Copies of the data can be obtained free of charge on application to CCDC, 12 Union Road, Cambridge CB2 1EZ, UK (fax: (+44) 1223-336-033; e-mail: deposit@ccdc.cam.ac.uk).

Acknowledgements

We thank the Deutsche Forschungsgemeinschaft (DFG; GL 300-1/4 and postdoctoral fellowship, O.M.) and US National Science Foundation for support, and Johnson Matthey PMC for a loan of rhodium.

[1] a) *Comprehensive Asymmetric Catalysis I–III* (Eds.: E. N. Jacobsen, A. Pfaltz, H. Yamamoto), Springer, Berlin, Germany, **1999**; b) *Catalytic Asymmetric Synthesis* (Ed.: I. Ojima), 2nd ed., Wiley-VCH, New York, **2000**.

[2] K. Muñiz, C. Bolm, *Chem. Eur. J.* **2000**, *6*, 2309.

[3] Reviews, perspectives, and commercial applications: a) A. Togni, *Angew. Chem.* **1996**, *108*, 1581; *Angew. Chem. Int. Ed. Engl.* **1996**, *35*, 1475; b) C. J. Richards, A. J. Locke, *Tetrahedron: Asymmetry* **1998**, *9*, 2377; c) A. Togni, N. Bieler, U. Burckhardt, C. Köllner, G. Pioda, R. Schneider, A. Schnyder, *Pure Appl. Chem.* **1999**, *71*, 1531; d) H.-U. Blaser, F. Spindler, Chapter 41.1 in ref. [1]; e) D. A. Dobbs, K. P. M. Vanhessche, E. Brazi, V. Rautenstrauch, J.-Y. Lenoir, J.-P. Genêt, J. Wiles, S. H. Bergens, *Angew. Chem.* **2000**, *112*, 2080; *Angew. Chem. Int. Ed.* **2000**, *39*, 1992.

[4] Lead references to ferrocene-based diphosphines with only planar chirality elements: a) J. Kang, J. H. Lee, S. H. Ahn, J. S. Choi, *Tetrahedron Lett.* **1998**, *39*, 5523; b) R. Kuwano, T. Uemura, M. Saitoh, Y. Ito, *Tetrahedron Lett.* **1999**, *40*, 1327; c) M. T. Reetz, E. W. Beuttenmüller, R. Goddard, M. Pastó, *Tetrahedron Lett.* **1999**, *40*, 4977; d) G. Argouarch, O. Samuel, H. B. Kagan, *Eur. J. Org. Chem.* **2000**, 2885; e) G. Argouarch, O. Samuel, O. Riant, J.-C. Daran, H. B. Kagan, *Eur. J. Org. Chem.* **2000**, 2893.

[5] a) H. Brunner, A. Winter, J. Breu, *J. Organomet. Chem.* **1998**, *553*, 285; b) T. Ohkuma, M. Kitamura, R. Noyori, Chapter 1 in ref. [1b].

[6] J. B. Lambert, Y. Zhao, R. W. Emblidge, L. A. Salvador, X. Liu, J.-H. So, E. C. Chelius, *Acc. Chem. Res.* **1999**, *32*, 183; see the section "effects beyond the β position".

[7] H. Brunner, *Angew. Chem.* **1999**, *111*, 1248; *Angew. Chem. Int. Ed.* **1999**, *38*, 1194.

[8] a) H. Brunner, J. Wachter, J. Schmidbauer, G. M. Sheldrick, P. G. Jones, *Angew. Chem.* **1986**, *98*, 339; *Angew. Chem. Int. Ed. Engl.* **1986**, *25*, 371; H. Brunner, J. Wachter, J. Schmidbauer, G. M. Sheldrick, P. G Jones, *Organometallics* **1986**, *5*, 2212; b) H. Brunner, M. Prommesberger, *Tetrahedron*: *Asymmetry* **1998**, *9*, 3231.

[9] F. Agbossou, E. J. O'Connor, C. M. Garner, N. Quirós Méndez, J. M. Fernández, A. T. Patton, J. A. Ramsden, J. A. Gladysz, *Inorg. Synth.* **1992**, *29*, 211.

[10] M. A. Dewey, Y. Zhou, Y. Liu, J. A. Gladysz, *Organometallics* **1993**, *12*, 3924.

[11] a) D. M. Dalton, C. M. Garner, J. M. Fernández, J. A.Gladysz, *J. Org. Chem.* **1991**, *56*, 6823, and earlier full papers therein; b) Y. Wang, J. A. Gladysz, *J. Org. Chem.* **1995**, *60*, 903; c) G. A. Stark, M. A. Dewey, G. B. Richter-Addo, D. A. Knight, A. M. Arif, J. A. Gladysz in *Stereoselective Reactions of Metal-Activated Molecules* (Eds.: H. Werner, J. Sundermeyer), Vieweg, Braunschweig, Germany, **1995**, pp. 51; d) O. Meyer, P. C. Cagle, K. Weickhardt, D. Vichard, J. A. Gladysz, *Pure Appl. Chem.* **1996**, *68*, 79.

[12] J. A. Gladysz, B. J. Boone, *Angew. Chem.* **1997**, *109*, 566; *Angew. Chem. Int. Ed. Engl.* **1997**, *36*, 550.

[13] a) W. E. Buhro, B. D. Zwick, S. Georgiou, J. P. Hutchinson, J. A. Gladysz, *J. Am. Chem. Soc.* **1988**, *110*, 2427; b) See also B. D. Zwick, M. A. Dewey, D. A. Knight, W. E. Buhro, A. M. Arif, J. A. Gladysz, *Organometallics* **1992**, *11*, 2673.

[14] a) Basicities of alkoxy ligands: S. K. Agbossou, J. M. Fernández, J. A. Gladysz, *Inorg. Chem.* **1990**, *29*, 476; b) nucleophilicities of amido ligands: M. A. Dewey, D. A. Knight, A. M. Arif, J. A. Gladysz, *Chem. Ber.* **1992**, *125*, 815.

[15] F. B. McCormick, W. B. Gleason, X. Zhao, P. C. Heah, J. A. Gladysz, *Organometallics* **1986**, *5*, 1778.

[16] Other literature relevant to points discussed below: a) M. J. Burk, *Acc. Chem. Res.* **2000**, *33*, 363; b) M. J. Burk, J. E. Feaster, W. A. Nugent, R. L. Harlow, *J. Am. Chem. Soc.* **1993**, *115*, 10125; c) I. D. Gridnev, N. Higashi, K. Asakura, T. Imamoto, *J. Am. Chem. Soc.* **2000**, *122*, 7183; d) S. Feldgus, C. R. Landis, *J. Am. Chem. Soc.* **2000**, *122*, 12714; e) C. R. Landis, J. Halpern *J. Am. Chem. Soc.* **1987**, *109*, 1746; f) W. Li, X. Zhang, *J. Org. Chem.* **2000**, *65*, 5871, and earlier work from this group therein.

[17] K. Kromm, J. A. Gladysz, unpublished results.

[18] a) B. D. Zwick, A. M. Arif, A. T. Patton, J. A. Gladysz, *Angew. Chem.* **1987**, *99*, 921; *Angew. Chem. Int. Ed. Engl.* **1987**, *26*, 910; b) see also B. D. Zwick, Ph.D. Thesis, University of Utah, **1987**.

[19] The non-racemic five- and six-membered chelates were synthesized from opposite enantiomers of **1**. For ease of comparison, the configurations of all complexes in the former series (and the hydrogenation products) have been inverted in the text, Tables, Scheme and Figures. The true configurations are designated in the Experimental Section.

[20] Chiral compounds not preceded by *R*/*S* descriptors are racemic. Rhenium configurations are designated by a modified Cahn-Ingold-Prelog system referenced in earlier papers.[11] Priority sequence for ligands in this study: (η^5-C_5H_4X) > PPh_2Rh > PPh_3 > PPh_2H > PPh_2 > OTs > NO > CH_2P > CH_3 > H.

[21] J. A. Ramsden, C. M. Garner, J. A. Gladysz, *Organometallics* **1991**, *10*, 1631.

[22] J. J. Kowalczyk, S. K. Agbossou, J. A. Gladysz, *J. Organomet. Chem.* **1990**, *397*, 333.

[23] Abbreviations: OTs = OSO_2-*p*-$C_6H_5CH_3$; NBD = norbornadiene; OTf = OSO_2CF_3.

[24] P. C. Cagle, O. Meyer, K. Weickhardt, A. M. Arif, J. A. Gladysz, *J. Am. Chem. Soc.* **1995**, *117*, 11730.

[25] J. J. Kowalczyk, A. M. Arif, J. A. Gladysz, *Chem. Ber.* **1991**, *124*, 729.

[26] P. Johnston, M. S. Loonat, W. L. Ingham, L. Carlton, N. J. Coville, *Organometallics* **1987**, *6*, 2121.

[27] a) D. P. Riley, R. E. Shumate, *J. Org. Chem.* **1980**, *45*, 5187; b) R. R. Schrock, J. A. Osborn, *J. Am. Chem. Soc.* **1971**, *93*, 2397.

[28] J. H. Merrifield, G.-Y Lin, W. A. Kiel, J. A. Gladysz, *J. Am. Chem. Soc.* **1983**, *105*, 5811.

[29] a) W. Tam, G.-Y. Lin, W.-K. Wong, W. A. Kiel, V. K. Wong, J. A. Gladysz, *J. Am. Chem. Soc.* **1982**, *104*, 141; b) J. Merrifield, C. E. Strouse, J. A. Gladysz, *Organometallics* **1982**, *1*, 1204; c) G. L. Crocco, K. E. Lee, J. A. Gladysz, *Organometallics* **1990**, *9*, 2819.

[30] J. H. Merrifield, J. M. Fernández, W. E. Buhro, J. A. Gladysz, *Inorg. Chem.* **1984**, *23*, 4022.

[31] G. L. Crocco, J. A. Gladysz, *J. Am. Chem. Soc.* **1988**, *110*, 6110.

[32] The following citations are restricted to reactions of neutral cyclopentadienyl complexes and anionic species that give a neutral metal hydride complex bearing a monosubstituted cyclopentadienyl ligand: a) P. Brun, P. Vierling, J. G. Riess, G. Le Borgne, *Organometallics* **1987**, *6*, 1032; b) T. C. Forschner, J. A. Corella II, N. J. Cooper, *Organometallics* **1990**, *9*, 2478, and earlier work from this group therein.

[33] One closely related example is the reaction of the iron bromide complex [(η^5-C_5H_5)Fe(CO)($PPh(OEt)_2$)(Br)] and $LiNEt_2$, which gives the hydride complex [(η^5-$C_5H_4NEt_2$)Fe(CO)($PPh(OEt)_2$)-(H)].[32a] A number of conceptually similar hydride migrations have been reported. See for example R. P. Hughes, S. M. Maddock, A. L. Rheingold, L. M. Liable-Sands, *J. Am. Chem. Soc.* **1997**, *119*, 5988.

[34] a) O. Meyer, A. M. Arif, J. A. Gladysz, *Organometallics* **1995**, *14*, 1844; b) T.-S. Peng, A. M. Arif, J. A. Gladysz, *J. Chem. Soc. Dalton Trans.* **1995**, 1857.

[35] a) S. Georgiou, J. A. Gladysz, *Tetrahedron* **1986**, *42*, 1109; b) S. G. Davies, I. M. Dordor-Hedgecock, K. H. Sutton, M. Whittaker, *J. Am. Chem. Soc.* **1987**, *109*, 5711.

[36] a) Conformations of $ReCH_2$-XRR′R″ linkages have also been studied.[34] Typically, the largest group (R″) gives a torsion angle of approximately 180°, such that the X–R″ bond is *anti* to the Re–C bond. Accordingly, (*S*)-**9** exhibits a Re-C1-P2-C50 torsion angle of −176.9°; b) for analyses of both conformational and configurational equilibria in related amido and alkoxide complexes, see M. A. Dewey, G. A. Stark, J. A. Gladysz, *Organometallics* **1996**, *15*, 4798. At equilibrium, the smallest group (R) prefers the position analogous to the phosphorus lone pair in crystalline (*S*)-**9**.

[37] a) T. Ireland, G. Großheimann, C. Wieser-Jeunesse, P. Knochel, *Angew. Chem.* **1999**, *111*, 3397; *Angew. Chem. Int. Ed.* **1999**, *38*, 3212; b) L. Schwink, P. Knochel, *Chem. Eur. J.* **1998**, *4*, 950.

[38] a) J. Kang, J. H. Lee, S. H. Ahn, J. S. Choi, *Tetrahedron Lett.* **1998**, *39*, 5523; b) J. J. A. Perea, A. Börner, P. Knochel, *Tetrahedron Lett.* **1998**, *39*, 8073.

[39] Many other phosphido complexes [(η^5-C_5H_5)Re(NO)(PPh_3)(PRR′)] are described in ref. [13]. However, a replacement of the PPh_3 ligand would necessitate a new resolution procedure.

[40] a) Y.-H. Huang, F. Niedercorn, A. M. Arif, J. A. Gladysz, *J. Organomet. Chem.* **1990**, *383*, 213; b) T.-S. Peng, C. H. Winter, J. A. Gladysz, *Inorg. Chem.* **1994**, *33*, 2534.

[41] a) P. Sauvageot, O. Blacque, M. M. Kubicki, S. Jugé, C. Moïse, *Organometallics* **1996**, *15*, 2399; b) C. Poulard, G. Boni, P. Richard, C. Moïse, *J. Chem. Soc. Dalton Trans.* **1999**, 2725.

[42] G. Helmchen, A. Pfaltz, *Acc. Chem. Res.* **2000**, *33*, 336.

[43] A. F. Burchat, J. M. Chong, N. Nielsen, *J. Organomet. Chem.* **1997**, *542*, 281.

[44] R. M. Herbst, D. Shemin in *Organic Synthesis Coll.*, *Vol. 2*, Wiley, New York, **1943**, pp. 1.

[45] B. D. Vineyard, W. S. Knowles, M. J. Sabacky, G. L. Bachman, D. J. Weinkauff, *J. Am. Chem. Soc.* **1977**, *99*, 5946.

[46] a) B. A. Andersson, *Acta Chem. Scand.* **1971**, *25*, 1514; b) Supelco Technical Bulletin 765G; Supelco Inc, Bellefonte, PA; one of nine references in this brief review: S. Nakaparskin, E. Gil-Av, J. Oro, *J. Anal. Biochem.* **1970**, *33*, 374.

[47] A privately manufactured column was employed, but equal or better separations would be realizable with commercial cyclodextrin fused silica capillary columns (e.g. FS-LIPODEX; Macherey-Nagel).

[48] a) See footnote [49] in ref. [13a]; b) G. M. Sheldrick, SHELX-93, University of Göttingen, **1993**. See also G. M. Sheldrick in *Crystallographic Computing 3* (Eds.: G. M. Sheldrick, C. Krüger, R. Goddard), Oxford University, England, **1993**, p. 175.

[49] D. T. Cromer, J. T. Waber in: *International Tables for X-ray Crystallography* (Eds.: J. A. Ibers, W. C. Hamilton), Kynoch, Birmingham, England, **1974**.

[50] H. D. Flack, *Acta Crystallogr.* **1983**, *A39*, 876.

Received: September 19, 2000 [F2742]